Review

Not peer-reviewed version

Biochar-Derived Persistent Free Radicals: A Plethora of Environmental Applications in a Lights and Shadows Scenario

Silvana Alfei * and Omar Ginoble Pandoli

Posted Date: 15 March 2024

doi: 10.20944/preprints202403.0855.v1

Keywords: Biochar (BC); pyrolysis; biochar-derived permanent free radicals (PFRs); reactive oxygen species (ROS); PFRs-mediated BCs applications; environmental risk

Review

Biochar-Derived Persistent Free Radicals: A Plethora of Environmental Applications in a Lights and Shadows Scenario

Silvana Alfei *and Omar Ginoble Pandoli

Department of Pharmacy (DIFAR), Viale Cembrano, 4, 16148, University of Genoa, Italy; omar.ginoblepandoli@unige.it (O.G.P.)
* Correspondence: alfei@difar.unige.it

Abstract: Biochar (BC) is a carbonaceous material obtained by pyrolysis at 200−1000 °C in the limited presence of O_2 of different vegetable and animal biomass feedstocks. BC has demonstrated great potential, mainly in environmental applications, due to its high sorption ability and persistent free radicals (PFRs) content. These characteristics enable BCs to carry out the direct and PFRs-mediated removal/degradation of environmental organic and inorganic contaminants. The types of PFRs possibly present in BC depend mainly on the pyrolysis temperature and the kind of pristine biomass. Since they also can cause ecological and human damage, a systematic evaluation of the environmental behavior, risks, or management techniques of BC-derived PFRs is urgent. PFRs generally could consist of a mixture of carbon- and oxygen-centered radicals, and of oxygenated carbon-centered radicals, depending on the pyrolytic conditions. Here, to promote a more productive and beneficial use of BC and related PFRs and stimulate further studies to make them environmentally safer and less hazardous to humans, we have first reviewed the most common methods used to produce BC, its main environmental applications, the primary mechanisms by which BC remove xenobiotics, as well as the reported mechanisms for PFRs formation in BCs. Secondly, we have discussed the PFRs environmental migration and transformation; we have reported the main PFRs-mediated applications of BCs to degrade inorganic and organic pollutants, the correlated environmental potential risks, and the possible strategies to limit them.

Keywords: biochar (BC); pyrolysis; biochar-derived permanent free radicals (PFRs); reactive oxygen species (ROS); PFRs-mediated BCs applications; environmental risk

1. Introduction

Biochar (BC) is a stable carbon-rich black solid produced from vegetable or animal biomass feedstocks when pyrolyzed. Pyrolysis is a procedure that involves the heating of substrates at 200-1000 °C under oxygen-limited conditions [1]. The term "biochar" derives from the combination of "bio-," which stands for "biomass," and "char," meaning "charcoal." In recent years, BC has received wide attention due to its potential application in carbon sequestration, soil amendment/remediation, wastewater treatment, and catalysis [2]. Batch and column sorption experiments have shown that certain types of BC have good adsorption performance for heavy metals, dyes, or phosphate from aqueous solutions and are being investigated as cost-effective, promising, and eco-friendly alternative adsorbent materials [3]. As a soil improver, BC can reduce soil acidity and help maintaining soil moisture and nutrient levels. Through its carbon sequestration action, BC performs climate restoration. Moreover, due to its strong adsorption capacity, BC can remove environmental xenobiotics, thus preventing their uptake in plants, animals, and humans [4–7]. Additionally, BC derived from thermal treatment of organic material generally contains persistent free radicals (PFRs) bound to the external or internal surfaces of its solid particles' [8,9]. Such BC-bound PFRs, which are reactive due to unpaired electrons, can persist for minutes and up to several months, in contrast to traditional transient radicals [10], thus conferring BC the capacity to degrade organic pollutants through the generation of other reactive oxygen species (ROS) and sulfate radicals [11–13]. In this context, BC-bound PFRs have been investigated to activate persulfate ($S_2O_8^{2-}$) to obtain sulfate radicals, which efficiently degraded phenolic compounds and polychlorinated biphenyls [14], acid orange 7 [15], and sulfamethoxazole [16,17]. In the presence of PFRs, hydrogen peroxide (H_2O_2) or oxygen (O_2) are activated to produce hydroxyl radicals (OH•) and superoxide radical ($O_2•^-$), which succeeded in efficiently degrading chloro-biphenyl [18], diethyl phthalate [19,20], and ciprofloxacin [21]. By the PFRs-mediated activation of peroxyl mono sulfate (PMS), radical species such as $SO_4•^-$, •OH, and $O_2•^-$, as well as non-radical species such as $^1O_2$ formed that were the main contributors to the degradation of antibiotics [22]. On the other hand, by stimulating the production of ROS, PFRs can inhibit seed germination and retard the growth of roots and shoots [23]. Additionally, the BC production itself may cause the release of xenobiotics such as polycyclic aromatic hydrocarbons (PAHs), toxic inorganic elements, and dioxins, thus posing potential risks to human health and the environment [1]. The scientific community should evaluate BC and BC-bound PFRs' positive and negative impacts before their extensive ecological applications. Although the environmental behavior and risks of BC and BC-associated PRFs are increasingly attracting the researchers' attention, in the last ten years, the study about their toxicity remains still very limited (96 publications), if compared to that concerning PFRs in general (542 publications) and their degradation capability (402 publications) (Figure 1).

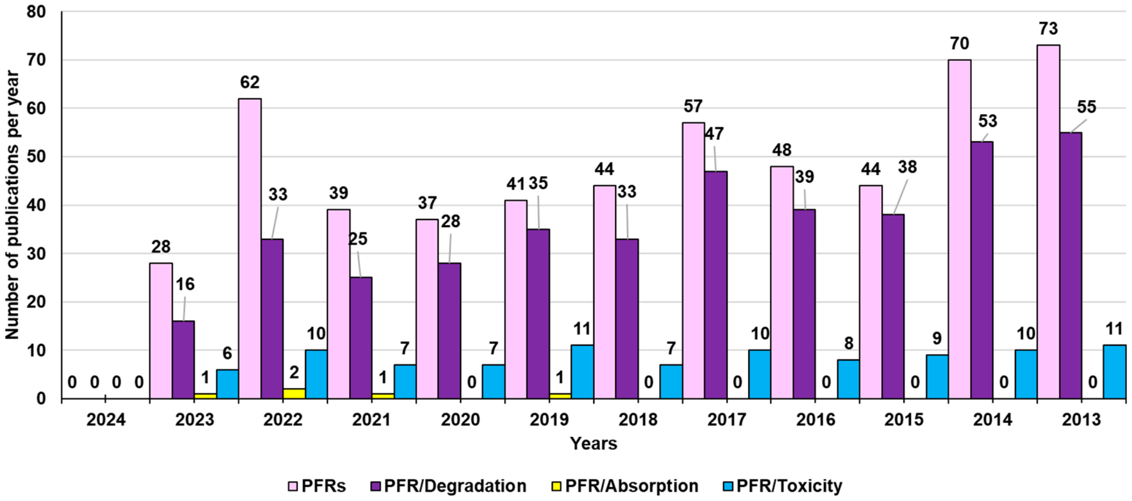

Figure 1. Number of publications on PFRs and their degradation, absorption, and possible toxic actions of the last ten years according to PubMed dataset. The survey was carried out using the following keywords: permanent free radicals (rose bars); permanent free radicals AND degradation (purple bars); permanent free radicals AND absorption (yellow bars); permanent free radicals AND toxicity (light blue bars).

However, to safeguard the environment from BC-related PFRs' potential adverse effects, it is necessary to comprehensively and systematically consider their environmental risks, formation mechanisms, and controlling factors [13], as well as the corresponding possible mitigation actions. Studies have shown that the type of biomass feedstock used to produce BC is pivotal in determining the physicochemical properties of the resulting BC, which also strongly affect the formation and characteristics of PFRs. To date, the types of biomasses used to prepare BC and involved in the investigation of BC-bound PFRs mainly include lignocellulosic biomasses (hemicellulose, cellulose, and lignin), such as pine needles, wheat straw, lignin, cow manure, rice husk, and maize straw [24–26]. Bamboo is an emerging starting material perfect for synthesizing BC and activated carbon (AC) due to its inexpensive cost, high biomass yield, and accelerated growth rate [27]. Anyway, only a few researchers and scientists have used bamboo as a unique source for developing BC so far, as established by the number of publications on bamboo-derived BC developed in the last ten years (331) vs. those on BC derived by different other sources (13630) (Figure 2).

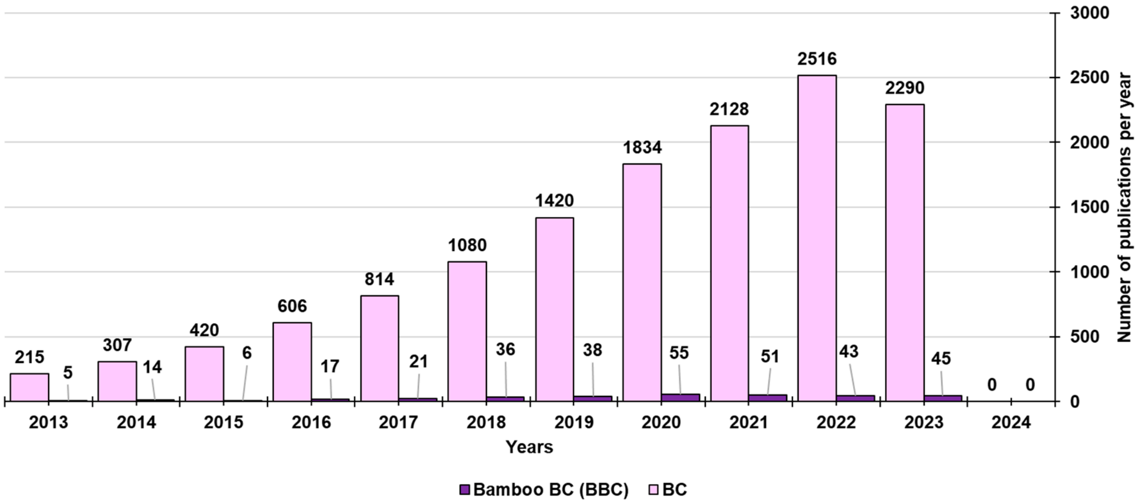

Figure 2. Number of publications on BCs and on bamboo-derived BCs in the last ten years according to PubMed dataset. The survey used the following keywords: biochar (rose bars) and bamboo biochar (purple bars).

Among the 331 publications on bamboo-derived BC, most parts were about their adsorption activity (119), followed by those on their degradation capacity (87). At the same time, few studies were conducted on their possible toxic action (Figure 3).

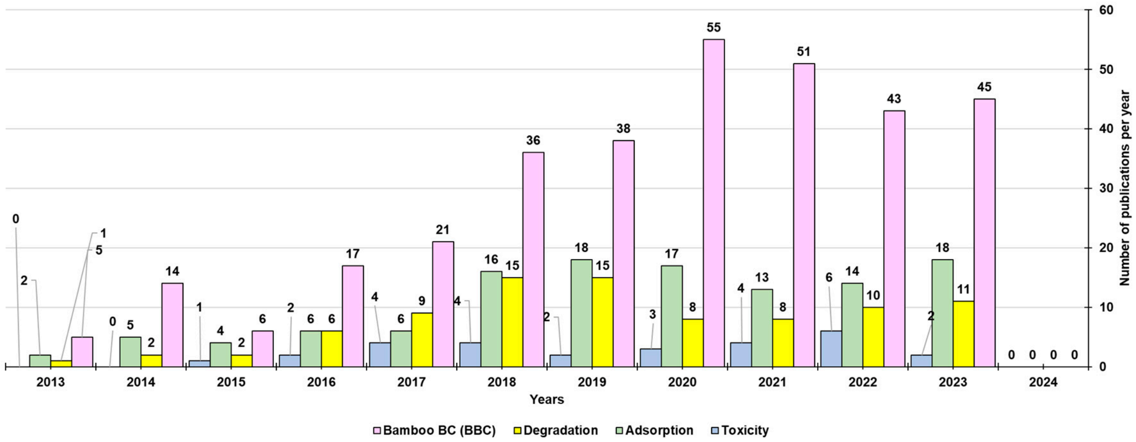

Figure 3. Number of publications on bamboo-derived BCs, as well as their absorption, degradation, and toxic properties of the last ten years according to PubMed dataset. The survey was carried out using the following keywords: bamboo biochar (rose bars); bamboo biochar AND adsorption (green bars); bamboo biochar AND degradation (yellow bars); bamboo biochar AND toxicity (light blue bars).

In this scenario, to promote a more productive and beneficial use of BC and related PFRs and stimulate further studies to make them environmentally safer and less hazardous to humans, we have first reviewed the most common methods used to produce BC, its main environmental applications, as well as the reported mechanisms for PFRs formation in BC. The main factors influencing the physicochemical properties of BC have also been reported. Secondly, we have discussed the PFRs environmental migration and transformation, the main PFRs-mediated applications of BC to remediate inorganic and organic pollutants described in the last five years, the correlated potential risks to the environment and humans, and the possible strategies to limit them.

2. Biochar (BC)

The constant growth in world population translates into a continued increase in the global energy requirement by all sectors and a dramatic decrease in fossil fuels, the primary energy source [28–30]. Furthermore, the effect of the CO_2 emissions on the environment determines additional global energy issues, which make the replacement of fossil fuels necessary and urgent [31]. In this regard, biochar (BC) mainly obtained from organic waste, and possessing the capability of sequestering carbon, represents a rich carbon source and an alternative to fossil fuels [32,33]. Table 1 report the biomasses commonly used for BC production [34–47].

Table 1. Main sources and general application of BCs.

Source biomass	Ref.	Applications	Refs.
Crop residue	[34]	Carbon sequestration	[48]
Kitchen waste	[35]		
Forestry	[36]	Soil amendment	[49]
Agricultural waste	[37]		
Sugar beet tailings	[38]	Composting	[50]
Forest residues	[39]		
Waste wood	[40]	Wastewater treatment	[51]
Bioenergy crops	[41]		
Municipal solid waste	[42]	Energy production/storage	[52]
Wheat straw	[43]	Adsorbing xenobiotics	[53]
Rice straw	[44]	Reducing greenhouse emission gas	[54]
Food manure	[45]	Xenobiotics degradation	[55]
Animal manure	[46]	Catalysis	[56]
Corn cob	[47]		

BC obtained by the combustion of biomasses reported in Table 1 have demonstrated to possesses nonpareil physicochemical properties such as large surface area, high porosity, presence of several functional groups, high cation exchange capacity (CEC), and long-term stability, etc. (Figure 4). Such properties make BC suitable for various applications, including but not only carbon sequestration, soil amendment, energy storage, catalysis [48–56] (Table 1). Additionally, BC is cost-effective, has an eco-friendly nature, and is endowed with reusability (Figure 4) [57,58]. Mainly, BC is increasingly gaining attention by many researchers as material to efficiently remove various environmental contaminants, including antibiotics, thus reducing the emergence of microbial resistance [53,55].

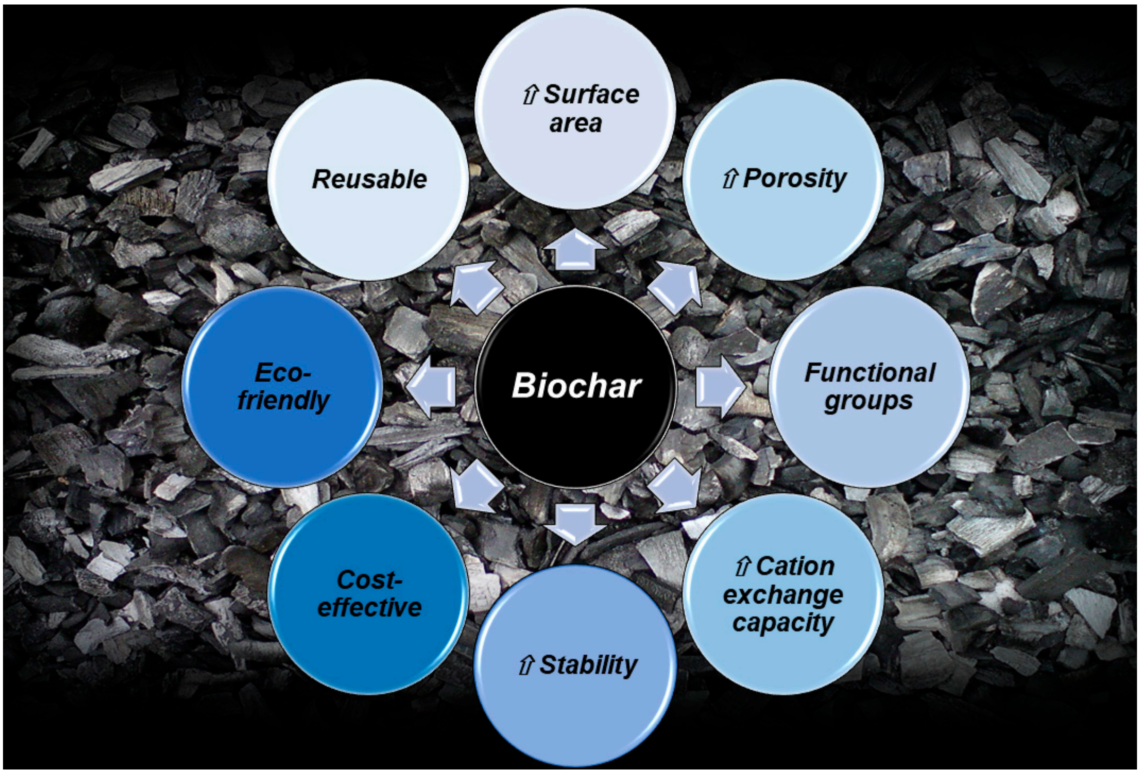

Figure 4. Some of the advantages and physicochemical properties of BCs.

Among the biomass waste materials appropriate for BC production, crop residues from agriculture, forestry, municipal solid waste, food, and animal manures have a high potential [59–64].

2.1. Main Methods to Produce Biochar

As reported in the following Table 2, BC can be quickly and fast prepared using thermochemical conversion techniques such as pyrolysis, hydrothermal carbonization, gasification, flash carbonization, and torrefaction [65,66], being pyrolysis the most adopted (Section 2.1.1).

Table 2. Main BC production methods, temperature conditions, and yields.

	Temperature (°C)	Residence Time	Biochar (%)	Bio-oil (%)	Syngas (%)	Refs
Pyrolysis	200–700	0.5-2 sec	35	30	35	[67]
	500–1000	Hours/day	12	75	13	
HC	180–300	1–16 h	50–80	5–20	2–5	[68]
Gasification	750–900	10–20 s	10	5	85	[69]
Torrefaction	290	10–60 min	80	0	20	[70]
Flash carbonization	300–600	< 30 min	37	--	--	[71]

HC = Hydrothermal carbonization.

2.1.1. Pyrolysis

Pyrolysis is a thermochemical process where the organic compounds present in the biomass are decomposed at a specific temperature [72]. Mainly, during pyrolysis, the thermal decomposition of organic materials occurs in an oxygen-free or oxygen-limited environment under the temperature range of 250-1000 °C [73]. In these conditions, the lignocellulosic components of biomass, such as cellulose, hemicellulose, and lignin, go through chemical reactions like depolymerization, fragmentation and cross-linking depending on the adopted temperatures. Three are the principal possible products, including solid, liquid, and gas physical state materials. The solid products comprise BC and ash, the liquid ones encompass bio-oils and tar, whereas the gaseous products (syngas) comprise carbon dioxide, carbon monoxide, hydrogen, and C1-C2 hydrocarbons [67]. As shown in Figure 5, during pyrolysis, the process parameters, including temperature, types and nature of biomass, residence time, heating rate, pressure, etc., could strongly affect BC's yield and its physicochemical characteristics [74,75]. Moreover, although BC derived from different biomasses are all entirely made of carbon content and ash, their elemental composition, as well as their physical characteristics and properties, could differ enormously based on the type of biomass, reaction conditions, and type of reactors used during the carbonization process [76] (Figure 5). Consequently, every experimental condition and the starting raw material should be considered for the proof-of-concept of the future industrial application of the BC.

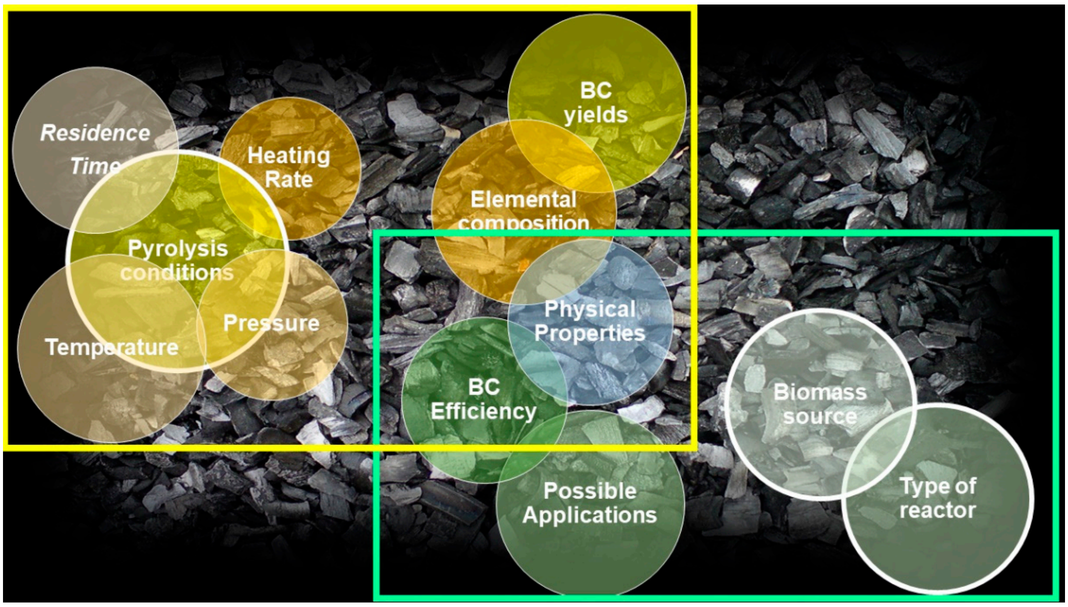

Figure 5. Parameters that mainly influence the pyrolysis process outcomes and the prepared BC elemental composition, physicochemical properties, and possible applications.

The most used reactors for the chemical transformation of different biomasses include paddle kilns, bubbling fluidized beds, wagon reactors, tubular ovens, and agitated sand rotating kilns. However, temperature remains the primary operating process condition that governs the yield in BC vs those of the oily and gaseous products. Usually, BC yield decreases, and syngas production increases when the pyrolysis temperature is improved [77]. Based on the heating rate, temperature, residence time, and pressure, pyrolysis can be categorized as fast or slow, as summarized in Table 3. Generally, fast pyrolysis is employed to maximize the liquid product yield, while slow pyrolysis is employed to maximize the solid product yield [78].

Table 3. Fast and slow pyrolysis details.

	Fast Pyrolysis	Slow Pyrolysis	Ref.
Target Product	Bio-oils	Biochar	[79]
Reactors	Bubbling fluidized bed Ablative reactor Rotary cone	Fixed bed pyrolysis reactor Auger pyrolysis reactor	
Warming rate	10-10000°C/min	0.1-10°C/min	
RT at ⇧ temperature	0.5-2 seconds	> 1 hour	
Aeration	Oxygen-free	Oxygen-free or limited	
Advantages	⇧ Yield of bio-oil	⇧ Yield of BC Accepted a wide range of particle size	

Disadvantages	⇓ BC yield Required fine particles of biomass feed (1-2 mm) Prefer biomass with low moisture content (<10%)	Further treatment of gases is needed due to high CO concentrations
Applications	⇧ Potential for energy applications	Improvement of soil quality

RT = Residence time; ⇧ = high, higher; ⇓ = low, lower.

2.2. Biochar Characterization and Main Properties

The characterization of BC aiming at determining its elemental composition, its surface functional groups, stability and structure is usually carried out employing various modern techniques such as Scanning Electron Microscopy (SEM), Transmission electron microscopy analysis (TEM), Elemental Analysis (EA*)*, Energy-Dispersive X-ray Spectroscopy (EDXS), X-ray Fluorescence spectroscopy (XRF), Fourier Transform Infrared Spectrometer (FTIR), Thermo Gravimetric Analysis (TGA), X-Ray Diffraction (XRD), Brunauer-Emmett-Teller (BET), Transmission Electron Microscopy (TEM), Nuclear Magnetic Resonance (NMR), Raman Spectroscopy, X-ray photoelectron spectroscopy (XPS), Electron Energy Loss Spectroscopy (EELS), Cation Exchange Capacity (CEC), and Electron Paramagnetic Resonance (EPR) or Electron Spin Resonance (ESR) spectroscopy [38]. Table 4 summarizes the analytical techniques typically used to characterize BC regarding their physicochemical, surface, and structural characterization.

Table 4. Techniques typically used to characterize BCs in terms of their physicochemical, surface, and structural characterization.

Biochar characterization techniques					
Physicochemical Characterization		**Surface Characterization**		**Structural/Molecular Characterization**	
Chemical	**Physical**	**Investigation**	**Technique**	**Investigation**	**Technique**
pH	Surface area (BET)	Morphology	SEM	Thermal behavior	TGA
Cation exchange capacity (CEC)	Size (nm) (TEM)	Functional groups	FTIR/Raman	Structural arrangements	XRD
Electrical conductivity	Bulk density	Surface elements	SEM, EDX, XFR	Aromaticity	NMR/Raman
	Pore size (BET)	Surface oxygen	Boehm titration	Free radicals	EPR/ESR

As mentioned, the source of feedstock and the heat treatment temperatures during preparation are two significant factors that determine the physiochemical properties of BC.

The properties of pristine biomass that mainly influence the related BC include moisture content, ash content, calorific value, percentage of lignin, cellulose, hemicellulose, fractions of fixed carbon, and volatile components [78]. High-yield BC with high porosity is achievable using biomasses owing more lignin and less cellulose. Additionally, the volatile component, water content, particle size, and shape of the original biomass can also affect the property of BC [78]. Table 5 reports the general chemical and physical features of BC, while Table 6 reports some characteristics of BCs produced from specific feedstocks at various production temperatures.

Table 5. Main chemical and physical features of BCs.

Properties		Discussion
Chemical properties	Atomic ratio	⇓ O/C and H/C ratio for untreated biomass
	Elemental composition	⇑ Carbon content (>95%) * ⇓ Hydrogen content (<5%) * ⇓ Oxygen content (<2%) *
	Energy content	⇑ Energy content with temperature (From 15-20 MJ/kg [a] to 30–35 MJ/kg [b] at 700 °C
	Fixed carbon (FC) ** Volatile matter (VM)	⇑ in FC (from 10% [a] to 90%[b] at 700 °C) ⇓ in VM (from 90% [a] to 10% [b] at 700°C)
	Structural composition	Partially decomposed cellulose [c] Near totally decomposed hemicellulose [c] Partially decomposed lignin [c] Release of O_2 and H_2 ⇓ Oxygenated functional groups in BC (OH and C=O groups) * ⇑ Highly stable aromatic structures in BC * (the maximum aromaticity at 500-800 °C) ⇑ Alkalinity and ability to neutralize acids in soils * ⇑ Unpaired negative charges that enable BC to accept protons
	pH value	⇑ pH-value (from 5-7.5 [a] to 10-12 [b] at > 500 °C) ⇑ Ash
	Cation exchange capacity (CEC)	⇑ CEC for BCs produced at relatively ⇓ low temperatures
	Ash content (SiO_2, CaO, K_2O, P_2O_5, Al_2O_3, MgO)	⇑ With temperature
	Self-heating degradation during storage	⇓ Highly volatile content in BC ⇓ Risk of self-heating ⇑ Thermal stability ⇓ Risk of spontaneous combustion ⇓ Water content and microbial
Physical properties	Density and porosity	⇑ Weight-based energy density * at ⇑ temperature ⇓ Bulk density * (the volume-specific weight of a bulk material in a heap or pile) ⇑ Porosities at ⇑ temperature
	Surface area	⇑ Total surface area * (< 800°C) ⇓ Total surface area * (> 800-1000°C)
	Pore volume distribution Pore size distribution	⇑ Total pore volume * with ⇑ temperature Macropores (1000–0.05 μm) Mesopores (0.05–0.002 μm) Micropores (0.05–0.0001 μm (more than 80% of the total pore volume)
	Hydrophobicity Water holding capacity (WHC)	⇑ Hydrophobicity ⇓ Affinity to water ⇑ Porosity and amount of water that can be absorbed
	Mechanical stability	⇓ Mechanical stability during carbonatization ⇓ Structural complexity during carbonization
	Grindability	⇑ Grindability compared to the parent material
	Thermal conductivity Heat capacity	⇓ Thermal conductivity in BC (from 1300 J/(kgK) [a] to 1000 J/(kgK) [b] at 500°C)

Electromagnetic properties	⇑ Conductivity ⇑ Electromagnetic shielding efficiency

* Depending on pyrolysis temperature: a higher degree of carbonatation at higher temperatures; ** after removing the volatile components, the carbon content that remains in the solid structure is called fixed carbon; [a]row biomass; [b]BC; [c]depending on biomass and pyrolysis temperatures involved (< 650 °C decomposes almost all of the holocellulose (cellulose and hemicellulose); the temperatures required for decomposing lignin are several hundred degrees higher than that for holocellulose; CEC: is defined as the amount of exchangeable cations (e.g., Ca^{2+}, Mg^{2+}, K^+, Na^+, NH_4^+) that a material can capture, which directly depends on the surface structure, and presence of functional groups providing surface negative charges; ⇧ = high, higher or increase; ⇩ = low, lower or decrease.

Table 6. Properties of BCs produced from various feedstocks at various production temperatures (adapted from [80]).

Feedstock	**Pyrolysis temp.**	**Yield**	**Ash**	**pH**	**C**	**H**	**O**	**N**	**Surface area**
	($^{\circ}$C)	(%)	(%)		(%)	(%)	(%)	(%)	(m^2 g ^{1})
Canola straw	400	27.4	–	–	45.7	–	–	0.19	–
Corn cobs	500	18.9	13.3	7.8	77.6	3.05	5.11	0.85	0.0
Corn stover	450	15.0	58.0	–	33.2	1.40	8.60	0.81	12.0
Corn stover	500	17.0	32.8	7.2	57.3	2.86	5.45	1.47	3.1
Cottonseed hull	200	83.4	3.1	–	51.9	6.00	40.5	0.60	–
Cottonseed hull	800	24.2	9.2	–	90.0	0.60	7.00	1.90	322.0
Fescue straw	100	99.9	6.9	–	48.6	7.25	44.1	0.64	1.8
Fescue straw	700	28.8	19.3	–	94.2	1.53	3.60	0.70	139.0
Oak bark	450	–	11.1	–	71.2	2.63	12.9	0.46	1.9
Oakwood	400–450	–	2.9	–	82.8	2.70	8.05	0.31	2.7
Orange peel	150	82.4	0.5	–	50.6	6.20	41.0	1.75	22.8
Orange peel	700	22.2	2.8	–	71.6	1.76	22.2	1.72	201.0
Peanut shell	300	36.9	1.2	7.8	68.27	3.85	25.89	1.91	3.1
Peanut shell	700	21.9	8.9	10.6	83.76	1.75	13.34	1.14	448.2
Peanut straw	400	28.2	–	–	42.90	–	–	1.50	–
Pine needles	100	91.2	1.1	–	50.87	6.15	42.27	0.71	0.7
Pine needles	700	14.0	2.2	–	86.51	1.28	11.08	1.13	490.8
Pine shaving	100	99.8	1.2	–	50.60	6.68	42.70	0.05	1.6
Pine shaving	700	22.0	1.7	–	92.30	1.62	6.00	0.08	347.0
Pinewood	700	–	38.8	6.6	95.30	0.82	3.76	0.12	29.0
Poplar wood	400	32.0	3.5	9.0	67.30	4.42	–	0.78	3.0
Rice husk	500	–	42.2	–	42.10	2.20	12.10	0.50	34.4
Saw dust	450	–	1.1	5.9	72.00	3.50	24.41	0.08	–
Saw dust	550	–	2.8	12.1	85.00	1.00	13.68	0.30	–
Soybean stover	300	37.0	10.4	7.3	68.81	4.29	24.99	1.88	5.6
Soybean stover	700	21.6	17.2	11.3	81.98	1.27	15.45	1.30	420.3
Soybean straw	400	24.7	–	–	44.10	–	–	2.38	–
Spruce wood	400	36.0	1.9	6.9	63.50	5.48	–	1.02	1.8
Spruce wood	525	–	4.7	8.6	78.30	3.04	–	1.17	40.4
Wheat straw	400	34.0	9.7	9.1	65.70	4.05	–	1.05	4.8
Wheat straw	525	–	12.7	9.2	74.40	2.83	–	1.04	14.2
Chicken litter	620	43-49	53.2	-	41.50	1.20	0.70	2.77	-
Poultry litter	350	54.3	30.7	8.7	51.07	3.79	15.63	4.45	3.9
Poultry litter	700	36.7	46.2	10.3	45.91	1.98	10.53	2.07	50.9
Tire rubber	200	93.5	15.0	-	74.70	6.38	3.92	-	-
Tire rubber	800	43.0	10.5	-	86.0	0.87	2.16	0.47	50.0

2.2.1. The Question of Temperature

As already reported, the pyrolysis temperature and feedstock greatly influence the physicochemical properties of BC, including pH, specific surface area, pore size, CEC, volatile matter, ash, and carbon content. CEC and volatile matter decrease with increasing pyrolysis temperature, whereas pH, specific surface area, ash, carbon content, and pore volume increase with the increase in pyrolysis temperature [81]. Increasing temperature also causes the decrease of the number of acidic functional groups, especially carboxylic functional groups, and causes the appearance of carbonylic functional groups and alkalinity [82]. Particularly, unpaired negative charges forming during pyrolysis at higher temperatures enable BC to accept protons [82]. Although BC’s alkalinity increases with higher pyrolysis temperatures, thus improving its capacity to neutralize acids in soils, lower temperatures are necessary to preserve functional groups and obtain BC with higher CEC [83]. Low water content in BC, which reduces the possible microbial activity promoting self-healing and degradation, is achievable at a higher temperature. However, the highly porous structure of BC obtained in such conditions causes the ready adsorption of moisture from the surroundings, thus increasing water content, re-enabling microbial activity, and contributing to self-heating and degradation [81].

During biomass decomposition to BC, the total surface area changes like the porosity due to the escaping of volatile gases and increases with increasing temperature [84]. In this regard, a large surface area affects CEC and water holding capacity (WHC). Curiously, during pyrolysis, the hydro-properties of initial biomass undergo several modifications depending on the pyrolysis temperature, which can translate into contradicting findings. Notably, with increasing temperature, due to a decrease in functional oxygenated groups and an increase in aromatic structure, the material’s affinity to water is altered, the hydrophobicity of BC becomes higher than that of pristine biomass, and its capacity to retain water should be lower. On the contrary, thanks to increased porosity that changes the amount of water that can be adsorbed, BCs produced at high temperatures can hold more water in their porous structure than BC prepared at lower ones [85].

The mechanical stability of biomass usually decreases during pyrolysis and correlates inversely with the porosity and directly to the density of the BC and temperature. The electric conductivity increases with higher thermal treatment, improving the graphitic carbons' crystallinity and the carbons-packed domains' density [86]. BC with high mechanical stability can be produced from feedstocks with high density and lignin content, making lignin, the constituent, more resilient to decomposition and loss of structural complexity. On the contrary, BC with higher grindability can be obtained by the torrefaction of biomass with a larger amount of hemicellulose (e.g., agricultural residues) compared to woody biomass. The decomposition of biomass to BC causes a reduction in its bulk density and an increase in its porosity and, therefore, a decrease in its thermal conductivity depending on the pyrolysis temperature. Concerning the electric properties of BC, the reduction in oxygenated functional groups and the appearance of conjugated double bonds cause an increase in conductivity and electromagnetic shielding efficiency, which make BC suitable as an additive in various composite materials (e.g., building materials such as cement). Further, the effectiveness of shielding against electromagnetic interference is enhanced concerning the pristine biomass.

2.3. Possible Biochar Applications

The various properties of BC reported above, including the high carbon content, larger surface area, well-developed porous structures, and the surface sufficiently enriched with functional groups, render it potentially pertinent for various applications. In Table 7, we have reported the current possible environmental BC applications.

Table 7. Main possible applications of BC.

Application	Mechanisms	Refs.
Climate change mitigation	Sequestering carbon in soil ⇓ CO_2 emissions into the atmosphere ⇓ NO_2 emissions ⇓ CH_4 emissions Tackling 12% of current anthropogenic carbon emissions	[54]
Soil improvement	⇑ Physicochemical and biological properties of soils ⇑ Water retention capacity of soil ⇓ Nutrient leaching ⇓ Acids in soils ⇑ Microbial population and microbial activity in soils Positive impacts on the earthworm population Preventing desiccation	[49]
Waste management	By pyrolyzing waste biomass *	[87]
Energy production	By conversion of waste biomass to BC by fast pyrolysis, thus providing liquid fuel (bio-oil)	[52]
Capturing contaminants	By adsorption of both organic pollutants and/or metal ions from soil and water	[53,55]
Composting	⇑ Physicochemical properties of composting ⇑ Composting microbial activities ⇑ Organic matter decomposition	[50]

* Including crop residues, forestry waste, animal manure, food processing waste, paper mill waste, municipal solid waste, and sewage sludge; ⇧ = high, higher, improved, enhanced; ⇩ = low, lower, reduced, decreased.

BC production could be an alternative to mitigate climate change by carbon sequestration in soil, thus retaining half of the carbon fixed in biomass during photosynthesis and reducing CO_2, NO_2, and CH_4 emissions [54]. Mainly, BC shows long-term stability in soil. The mean carbon residence time in BC has been estimated to be around 90-1600 years, depending upon the labile and intermediate stable carbon components [54]. Due to these characteristics, BC can sequester carbon in soil, thus decreasing carbon dioxide emissions into the atmosphere and those of nitrous oxide and methane by biotic and abiotic mechanisms [54]. Experiments have demonstrated that emissions of greenhouse gases (including CH_4 and N_2O) can be avoided by pyrolyzing waste biomasses [88]. Concurrently, the pyrolysis process balances fossil fuel consumption by producing bioenergy.

Interesting, BC has been estimated to be capable of tackling 12% of current anthropogenic carbon emissions. Furthermore, thanks to its high carbon content, BC can work as a soil conditioner, mainly by improving soil's physicochemical and biological properties. BC increases soil water retention capacity by ~18%, reduces nutrient leaching [49], and neutralizes acidic soils, thus enhancing plant productivity, seed germination, plant growth, and crop yields. Additionally, wet BC prevents the soil desiccation [49]. While it has been reported that soils treated with BC demonstrated improved microbial population and activity [89], null or positive effects were observed in the earthworm population in soils amended with wood-based BC [90].

The production of BC itself is an economical and mutually beneficial strategy to manage and eliminate waste from animals and plants and reduce the pollution associated with it [89]. Furthermore, when waste biomass deriving mainly from animal manure and sewage sludge is pyrolyzed, the hazardous microbial population possibly present is killed, thus reducing its possible negative impact on the environment and humans. Unfortunately, toxic heavy metals from sewage sludge and municipal solid waste could persist in BC, which must be carefully checked and handled correctly before long-term soil application [91].

A remarkable potential use of BC, still too little investigated and controversial, is the production of bioenergy, as an alternative to fossil fuel, that could lower carbon emissions. In this regard, while slow pyrolysis allows a lower yield of liquid fuel and more BC, fast pyrolysis provides more liquid fuel (bio-oil) and less BC [92]. Evidence has demonstrated that BC can be successfully applied in environmental remediation because it is capable of adsorbing both organic and inorganic contaminants, such as pesticides, herbicides, PAH, dyes, and antibiotics, as well as non-biodegradable metals ions, that are highly toxic to all living organisms [53,55]. BC can enhance the composting process by improving its physicochemical properties and microbial activities and promoting the decomposition of organic matter. Also, more investigations are needed to evaluate BC compost's agricultural/environmental performance [50]. Table 8 summarizes some advantages and disadvantages associated with the production and use of BC.

Table 8. Advantages and disadvantages associated with the production and use of BC.

Advantages	Disadvantages
Obviate to significant modification on Earth	Gaseous aerosol emissions during improper pyrolysis
Enhanced soil productivity	Environmental pollution from dust, erosion and leaching of BC particles
Higher food security	Ash could be at risk for respiratory diseases.
Solution of xenobiotics danger	BC can sequester water and nutrients no further available for crops
Addressing waste management	Not desired sorption of residual herbicides and pesticides
Reduced utilization of fossil fuels	Long-term removal of crop residues for producing BCs can reduce overall soil health by diminishing the number of soil microorganisms and disrupting internal nutrient cycling
Less expensive than activated carbon (AC)	Possible negative impact on soil biota
Improvement of living microbiology in soil	Short-term adverse effects on earthworm population density
Greater WHC than AC Enhanced food web in soil Improved aeration in the soil Reduced loss of nutrients through leaching	No universal reduction in nitrous oxide emissions

AC = Activated carbon; WHC = water holding capacity.

As evidenced in Table 8, we are reimbursed with additional advantages by producing BC from biomass, including waste biomass. The cost necessary to produce BC is six-fold lower than that of commercially available activated carbon (AC), which, unlike BC, is deprived of some properties of BC, such as its ion exchange capacity [93]. Generally, BC does not require further processing to be activated, and thanks to its non-carbonized fraction and maintained oxygen-containing groups, such as carboxyl, hydroxyl, and phenolic surface functional groups, BC is capable of adsorbing both organic as well as inorganic contaminants, and to interacts with soil contaminants [53,55]. BCs produced from sewage sludge and manure have a high nutrient content for soils, thus enriching their quality [49]. Anyway, apart from the advantages of using BC, there is a series of possible fallouts, as reported, that need consideration. Among these, long-term removal of crop residues, like stems, leaves, and seed pods, for producing BC could reduce the overall soil health by diminishing the number of soil microorganisms and disrupting internal nutrient cycling with a possible negative impact on soil biota, including short-term adverse effects on earthworm population density. In this scenario, there is a dire need for further extensive research so that any possible issues associated with its usage can be aptly resolved.

2.3.1. Xenobiotics Removal by Biochar (BC)

As reported in the previous section, BC is a porous material, and its porosity, depending on the production temperature, allows it to interact with water nutrients and other materials, including inorganic metal cations and organic pollutants. Due to its enhanced porous structure, surface area, functional groups and mineral components, BC is an optimal absorbent material for solutions. Although BC produced through pyrolysis, has a relatively moderate adsorption capacity (3.6 g/g – 6.3 g/g for BC prepared at a temperature range of 300–700 °C) [94], it can be enhanced by modifying its physicochemical properties through acid, alkali, or oxidizing treatments, while the surface area can be altered mainly using acid treatments [95–97]. As an adsorbent, BC can absorb organic and inorganic contaminants such as PAH, and phthalate acid esters, and its help in improving the treatment of sewage wastewater containing organic xenobiotics has been widely reported [98]. In this context, several are the main mechanisms used by BC for capturing inorganic or organic pollutants, which have been included and discussed in Table 9.

Table 9. Main mechanisms by which BC can capture inorganic or organic contaminants.

Capturing Mechanism	Influencing factors #, Details °, Examples §	Ref.
Sorption *	⇑ Surface area # Microporosity of BC # pH #	[98]
Hydrogen bond formation **	For polar compounds °,**	
Electrostatic attraction/repulsion	For cationic compounds ° Interaction between positively charged cationic organic contaminants and negatively charged BC surfaces °,**	
Electrostatic outer sphere complexation	Due to metallic exchange with K^+ and Na^+ available in BC °,**	
Hydrophobic interactions ***	For non-polar compounds °	
Diffusion	Non-ionic compounds can diffuse into the non-carbonized and carbonized fractions of BC °	
Formation of surface complexes **	pH # Ionic radius # Between metal cations and -OH, -COOH on BCs °	
Precipitation	Lead precipitates as lead-phosphate-silicate in BC § Co-precipitates and inner-sphere complexes can form between metals and organic matter/mineral oxides of BC §	

* From water/soil onto biochar; ** for BCs produced at relatively lower temperatures; *** for BCs produced at higher temperatures; ⇑ = high, higher, improved, enhanced.

Interesting, BCs produced at higher temperatures exhibited higher sorption efficiency for the remediation of organic and metallic contaminants in soil and water. Additionally, it is worth mentioning that the sorption of organic xenobiotics by BC is more favored than that of inorganic ones. Concerning complexation with metal cations, the smaller is the ionic radius of metals, the greater will be the adsorption capacity by BC.

2.3.2. Not Only Adsorption

It is reported that the principal mechanism by which BC removes toxic heavy metals and other contaminants, including organic pollutants, is adsorption. Its adsorptive efficiency mainly depends on the type and number of functional groups, surface area, CEC, etc. Anyway, previous research studies and reviews on BC have evidenced the presence on the surface or inside its particles, of free radicals known as persistent free radicals (PFRs), whose nature depends strongly on the pyrolysis conditions and whose formation and characteristics mainly differ based on the feedstock types. In this regard, several recent studies have mainly focused on the role of BC-related PFRs in the degradation of organic xenobiotics, in addition to their adsorptive capacity. Odinga et al., in their recent work, reviewed the application of BCs-derived PFRs in environmental pollution remediation [13], while Fang et al. investigated the reactivity of PFRs in BC and their catalytic ability to activate persulfate to degrade pollutants [14]. On the other hand, Odinga et al. also considered and commented on the possible environmental risks of PFRs from BCs, which represent the shadows associated with these chemicals and need further study, knowledge, and regulation before their extensive application [13].

3. Biochar-Derived Free Radicals

As previously mentioned, BC has a broad prospective use in the treatment of environmental xenobiotics, in soil amendment, in photocatalytic and photothermal systems, for photothermal conversion, as electrical and thermal devices, as 3D solar vapor-generation devices for water desalination [99–102]. All these potentials are due to its high surface area and rich pore structure, which determines great physical absorptivity. They also depend on the chemical characteristics of BC, including the presence of PFRs [103,104]. In this regard, it is of paramount importance to clarify the formation mechanism of the free radicals in BC for the optimal management of their properties and their more efficient and safer utilization [105].

3.1. Persistent Free Radicals (PFRs)

An atom or molecule with at least a lone pair of electrons is a chemical species characterized by significant instability and high chemical activity and is referred to as a free radical species [88]. Usually, free radicals are highly unstable and rapidly react with each other, thus destroying as soon as they form, with a consequent very short half-life. Whereas, it has been found that in BC, some free radicals named persistent free radicals (PFRs), like the radicals that naturally occur in the environment known as environmental persistent free radicals (EPFRs), can remain stable for months and play a crucial role in subsequent reactions of oxidative degradation carried out by BC containing them [11,88,106,107] (Figure 6).

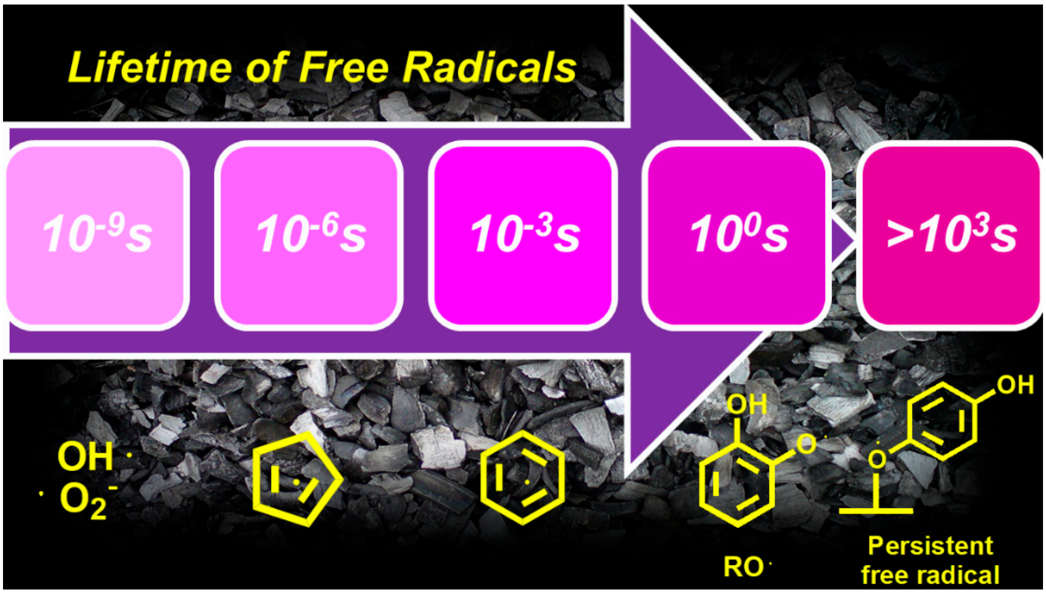

Figure 6. The lifetime of different free radicals.

Unlike other free radicals, PFRs are resonance-stabilized since they are bound to the external or internal surface of solid particles of BC. They can be analyzed by electron paramagnetic resonance spectroscopy (EPR) [11]. Figure 7a provides an example of EPR analysis of PFRs present on a solid N-doped hydro char prepared in a tube furnace at a temperature of up to 600 °C for 1 h under N_2 atmosphere [108].

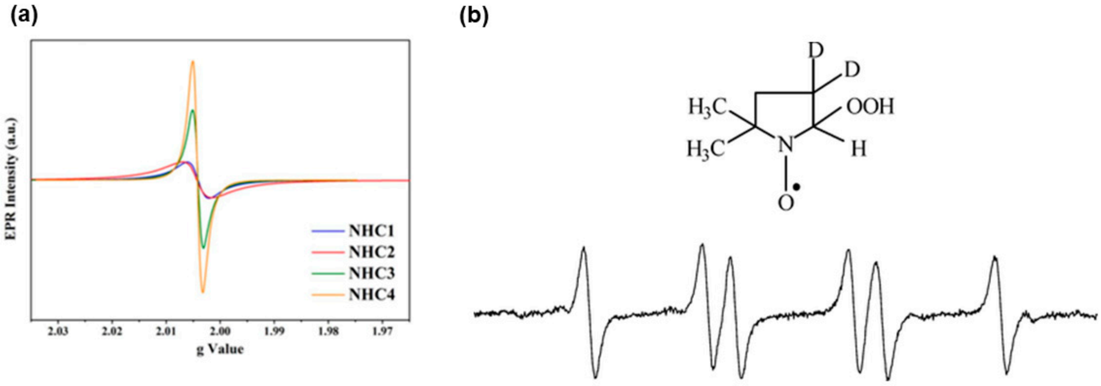

Figure 7. EPR analysis of PFRs generated on a N-doped hydro char prepared in a tube furnace to 600 °C for 1 h under N_2 atmosphere (a) [108]; EPR spectrum of the unstable free radical superoxide ($O_2{\bullet}^-$) when trapped by DMPO to form a long-lived nitroxide (DMPO–OOH) (b).

Their lifetime under vacuum appears infinite, while they react with molecular oxygen in the air, resulting in decay with time and simultaneous production of reactive oxygen species (ROS). In this regard, PFRs act as transition metals like Fe^{2+}, stimulating ROS production in aqueous systems. Unlike PFRs, ROS are detectable by EPR only when captured by a proper radical scavenger as 5,5-dimethyl-1-pyrroline-N-oxide (DMPO). Figure 7b provides an example of the EPR spectrum of the unstable free radical superoxide ($O_2{\bullet}^-$) when trapped by DMPO to form a long-lived nitroxide radical (DMPO–OOH). As in BC, by the EPR technique, PFRs were previously detected in combustion-generated particulate matter (PMs), sediments, and soils. PFRs are categorized into three classes, i.e., oxygen-centered PFRs (OCPFRs), carbon-centered PFRs (CCPFRs), and oxygenated carbon-centered radicals (CCPFRs-O). The EPR analyses provide three parameters: the PFRs concentration, the g-value, and the line width [88] (Figure 8).

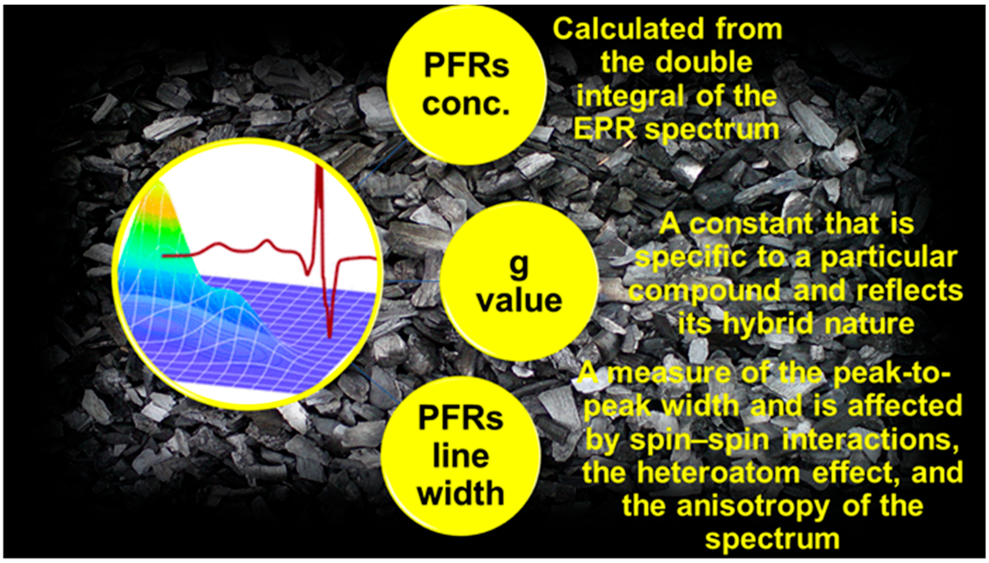

Figure 8. Information deriving from EPR analyses.

PFRs concentration is calculated from the double integral of the EPR spectrum and can reflect the content of PFRs in BC [109]. The g-value of PFRs is a constant specific to a particular compound, reflects its hybrid nature, and provides information about the type of radical [110]. The PFRs line width in the EPR spectrum measures the peak-to-peak width. It is affected by spin–spin interactions (including electron–proton interaction and electron–electron interaction), the heteroatom effect, and the anisotropy of the spectrum [88].

The line width reflects the relaxation time of spinning electrons [111]. It has been reported that the oxidation processes that can occur using BCs mainly depend on PFRs and these parameters [106,112,113]. These parameters are, in turn, affected significantly by pyrolysis conditions, biomass types, the elemental composition of pristine biomass, and the presence of external transition metals (Table 10).

Table 10. Factors influencing PFRs formation in BC.

Parameter	Influencing Factors	Specifications	Observations	Ref.
PFRs concentration	Biomass type	Cow manure, rice husk, others (< 500°C)	≠ Concentrations	[114,115]
		Non-lignocellulosic biomass with ⇓ H/C and O/C	⇓ Concentration	[116]
		Lignocellulosic biomass	⇑ Concentration	
	Temperature	300°C, 700°C	≠ Concentrations	[114]
		Maximum concentration at 600°C		[117]
		Maximum of concentration at 500-600°C		[10,118]
	Transition metals	Adsorb onto biomass and transfers electrons from polymer to metal center during pyrolysis	⇑ Concentration	[18]
Type of PFRs	Temperature	200-300°C	Oxygen centered radicals	[10]
		400°C	A mixture of oxygen and carbon-centered radicals	
		500-700°C	Exclusively carbon centered radicals	

Qin et al. [114] found that the PFR concentrations in the same BC obtained at different temperatures and in different kinds of BC obtained at the same temperature were significantly different. Tao et al. [117], as well as Xiang [118] and Huang et al. [10], found that in BCs by different feedstocks, the PFRs concentration first increased with increasing temperature, reaching a maximum around 500-600°C and then decreased with further increase of temperature. The relations between the feedstocks' properties or the BCs' composition with the PFRs concentration were also demonstrated [115], and non-lignocellulosic-biomass produced lower PFRs concentrations than lignocellulosic-biomass under the same pyrolytic conditions, perhaps due to their lower H/C and O/C atomic ratios [116]. The types of PFRs that can be produced during pyrolysis change during the pyrolysis process and with a temperature rise, as reported in Table 10. The study speculated that the reduction in oxygen content during biomass pyrolysis may account for the progressive conversion of oxygen-centered radicals to carbon-centered radicals [116].

3.1.1. Mechanism Proposed for PFRs Formation during Biomass Pyrolysis

The several environmental sources of PFRs include atmospheric particulate matter (PM), contaminated soil, materials from thermal treatments of plastic and hazardous waste, tar balls, products of pyrolysis of biodiesel and biomass waste feedstocks at high temperatures [11]. Concerning BC-derived PFRs, it was observed that they mainly form in the post-flame and cool-zone regions of combustion systems and other thermal conversion processes. Although the actual mechanism by which PFRs form during pyrolysis remains not fully clarified, transition metals capable of electron transferring and substituted aromatics molecules present in lignin have been recognized as critical factors of PFRs formation. Anyway, high concentration of PFRs have been detected also in the product of combustion of non-aromatic cellulose in absence of transition metals

[117]. Based on the temperature of pyrolysis processes, during the production of BC highly heterogeneous composite structures, comprising both labile and recalcitrant organic molecules, such as PAH, furans, and dioxins, as well as inorganic fractions, including oxides, cations, anions, and free radicals occur [119]. These fractions, products of incomplete combustion od biomass, may gradually form PFRs by different pathways including or not transition metals. As formed PFRs could be either only surface-stabilized or surface-stabilized in metal-radical complexes [13]. Generally, the breaking of covalent bonds by heat, light, electricity, and chemical energy possibly sustained by transition metals is essential to form free radicals, and during the pyrolysis process of biomass, its main constituents that are cellulose, hemicellulose, and lignin, undergo different reaction pathways at various destructive pyrolysis temperatures of 300 °C, 300–400 °C, and 350–450 °C. Figure 9 attempts to describe the possible series of events occurring during the biomass pyrolysis which could lead to the PFRs' formation and that are chemically described in Scheme 1 (concerning lignin) and Scheme 2 (concerning cellulose and emicellulose).

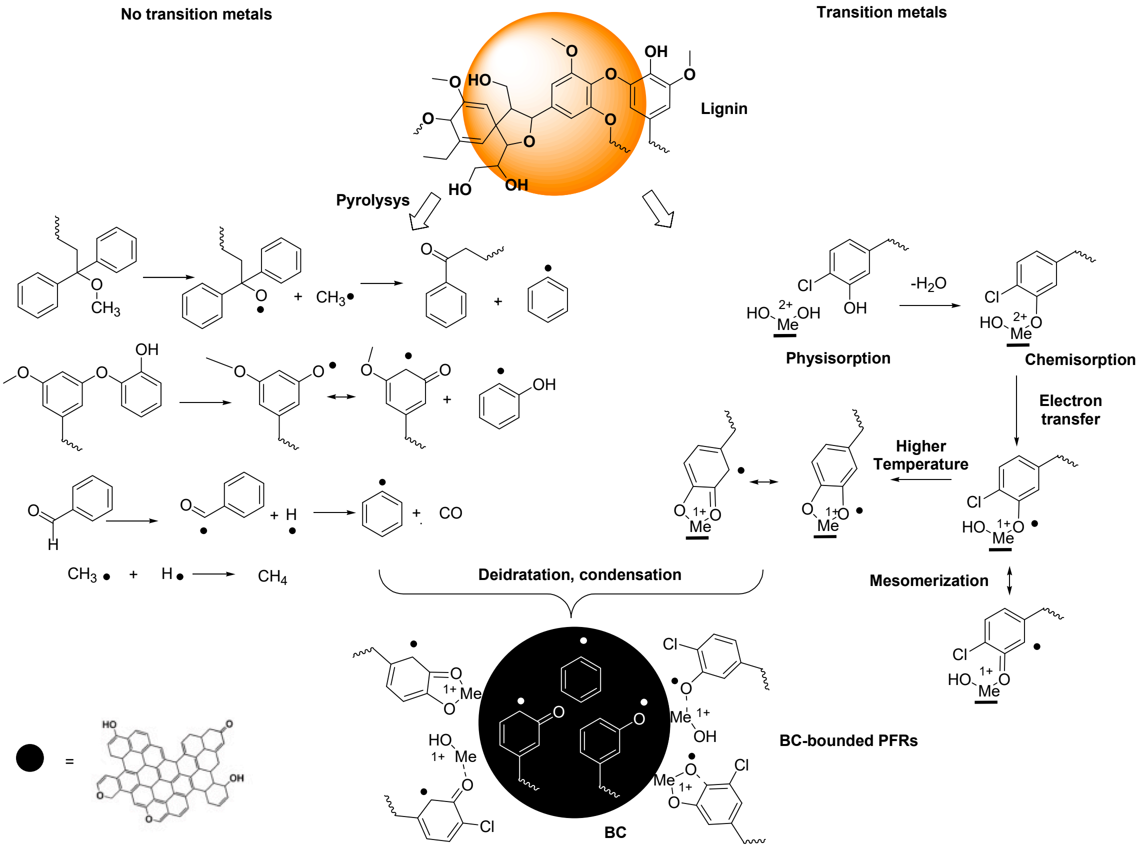

Scheme 1. Possible mechanisms leading to the formation of BC-bounded PFRs from lignin. The orange sphere represents biomass, while the black sphere represents BC whose hypothetic structures depending on pyrolysis condition have been shown at the bottom of the Scheme.

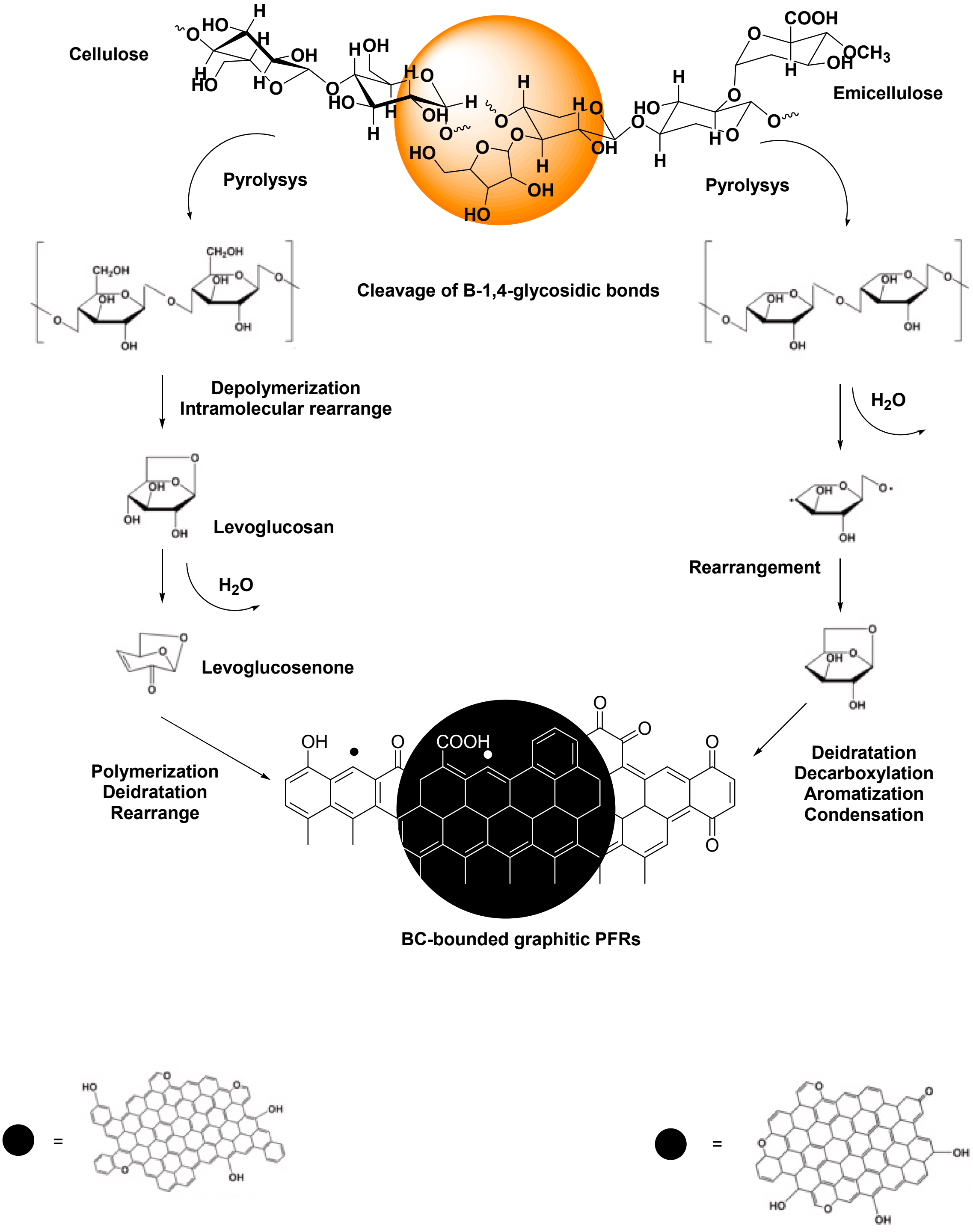

Scheme 2. Possible mechanisms leading to the formation of BC-bounded graphitic PFRs from cellulose (left side) and emicellulose (right side). The orange sphere represents biomass, while the black sphere represents BC whose hypothetic structures depending on pyrolysis condition have been shown at the bottom of the Scheme.

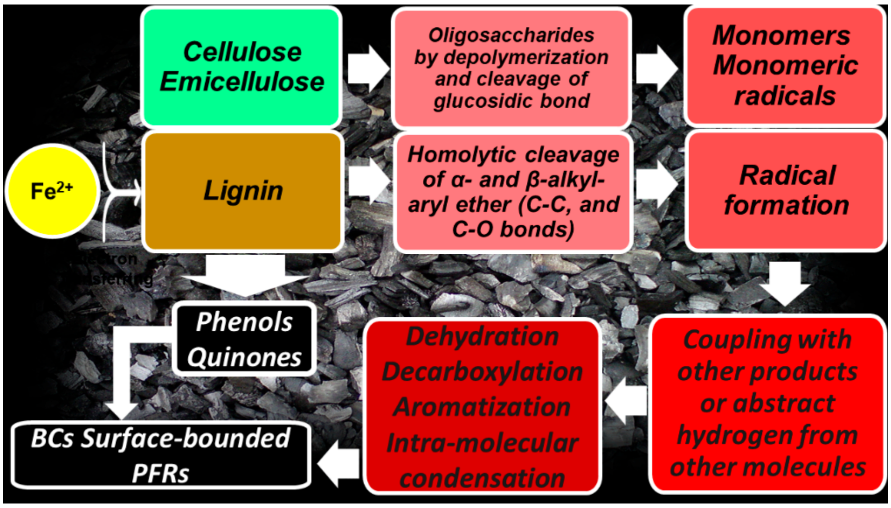

Figure 9. PFRs formation process.

First, the C-O and C-C covalent bonds of constituents of lignin vie electron transfer by transition metals or not are broken under heat to form free radical fragments, phenols, chinones, and other products of incomplete combustion. Simultaneously, the cleavage of glucoside bonds of cellulose and hemicellulose present in biomass feedstocks occurs causing depolymerization and formation of other radicals. These first radicals can couple to form bio-oil, pyrolysis syngas (CO_2, CO, CH_3CH_3 and CH_4), and BC simultaneously or abstract hydrogen from other molecules forming further radicals [115,120]. Several chemical reactions can occur including dehydration, decarboxylation with further emission of CO_2, CO and H_2O, aromatization, intra-molecular condensation leading to the formation of the crystalline graphene structure and graphitic radicals. During pyrolysis, the elemental composition of biomass undergoes changes that cause mutations in the types of radicals that, upon entrapment onto the BCs' surface, and/or formation of metals-radical complexes form stable PFRs [10].

According to what reported in literature, the possible types of PFRs comprise (i) transition metal mediated PFRs or (ii) PFRs inside organic matrices forming during biomass pyrolysis to give BC [121]. The transition metal mediated PFRs formation starts with the initial physisorption of an aromatic substituted molecule or of its degradation intermediate radicals generated at 150-400 °C or under UV irradiation onto the transition metal oxides such as ZnO, NiO, CuO, Fe_2O_3, and TiO_2 or transition metal ions [122]. Then, a chemisorption occurs by forming a chemical bond eliminating water or hydrogen chloride. Finally, a single electron is transferred from substituted aromatics to the center of transition metals, leading to the simultaneous reduction of metal and forming PFRs [122], whose stability is attributed to the synergy of metals and aromatic compounds [122]. Transition metal accepts an electron, and its valence changes from high to low during this process.

Unlike PFRs discussed previously, PFRs formed inside the matrix of organic moieties are not related to the presence of transition metals [121]. Still, they are highly dependent on the organic matter, while their concentration is significantly and positively correlated with the elemental carbon content [121]. In this case, PFRs are compared in thermally treated particles, and the breaking of chemical bonds in the precursor molecules during pyrolysis is the primary reason. At the initial pyrolysis stage, the homolytic cleavage of weak linkage bonds like the α- and β-alkyl aryl ether bonds, C-C, and C-O linkage resulted in forming free radicals in BC. The outer-surface free radicals would rapidly react and dissipate, resulting in a decrease in EPR signals. The free radical concentrations then increased with the extended pyrolysis and during the cooling stage, thus accumulating many free radicals on the BC surface [121] and dramatically growing the EPR signals. The free radicals formed in the matrix of the produced BC are probably protected from reacting with each other or other chemicals and thus stabilized.

As above mentioned, the type of biomass and its elemental composition, the presence of oxygenated functional groups, the pyrolysis conditions (temperature, heating time, and heating rate), and the presence of external transition metal as well as phenolic compounds strongly affect both the concentration, structure, and type of PFRs present in BC. Notably, no radical is produced during the first stage of pyrolysis, providing the transition char (< 300 °C). Subsequently, in the second stage of pyrolysis (300-500 °C), amorphous char is produced, and oxygen-centered radicals and oxygenated carbon-centered radicals appear. In the third stage of pyrolysis at 500-700 °C, composite char is created where the concentration of PFRs, including carbon-centered and oxygenated carbon-centered radicals, drastically decrease. Finally, when turbostratic char is produced (> 700 °C) little or no PFRs are further produced [13]. In the EPR, the g-factor values, even if they could change due to the presence of metal ions and temperature changes, are specific for a type of radical. Table 11 reports the main types of radicals recognizable in BC and their specific g-values.

Table 11. Features and g-values of the main PFRs forming in BC.

Radicals	g-value	Features
Carbon-centered radicals	< 2.003	Susceptible to oxidation in air
Carbon-centered radicals adjacent to an oxygen atom (oxygenated carbon-centered radicals)	2.003–2.004	Susceptible to oxidation in air
Oxygen-centered radicals	> 2.004	More stable in an atmospheric environment
Semiquinone radicals (oxygen-centered)	> 2.0045	More resistant to react with molecular oxygen in ambient environment
Phenoxy radicals (oxygenated carbon-centered radicals)	2.0030–2.0040	Susceptible to oxidation in air
Cyclopentadienyls (carbon-centered radicals)	< 2.003	Susceptible to react with molecular oxygen in ambient environment

3.2. PFRs: Lights and Shadows

3.2.1. PFRs Lights

It has been demonstrated that PFRs originating in BC by combustion in the presence or absence of external transition metals could play a vital role in several beneficial reactions, such as PFRs-mediated remediation and degradation of organic and inorganic pollutants by different actions and mechanisms, including oxidative and reductive processes (Table 12).

Table 12. Main actions and mechanisms by which PFRs remediate/degrade environmental xenobiotics.

EPFRs actions	Degraded substances *	Mechanism	Refs.
Activation of H_2O_2 by single electron transferring	SMX, CIP, SMT, TC, OG, MNZ, ERF benzene	Oxidation by the production of ROS ($OH\bullet\#$, $HO_2\bullet$, $O_2\bullet^-$)	[18,123]
Activation of O_2 by single electron transferring	Degradation of organic compounds Chloro-biphenyl Phenolic compounds Polychlorinated biphenyls Diethyl phthalate Thiacloprid Bisphenol A	Oxidation by the production of radical superoxide ($O_2\bullet^-$)	[7,11] [19,104]
Activation of persulfate ($S_2O_8^{2-}$)	X-3B, SMT, CTC, SMX, TC, MB, SDZ, OG	Oxidation by the production of sulfate radicals ($SO_4{}^{-}\bullet$)	[123]

Direct activity of macromolecular radicals on the BC surface	Direct degradation of organic chemicals	Oxidation	[55]
Direct activity of semiquinone-type radicals	As (III) removal	Oxidation	[124]
Direct activity of PFRs	Removal of Cr (VI)	Reduction to Cr (III)	[125–129]
Catalytic effects	Detoxification of environmental xenobiotics	Generation of activated species Stimulation of the microbial biotransformation	[55]
Ions' exchange	Enhancement of agricultural soil performance	Maintenance of CEC in soils	[130]
Electron-hole pair formation	Photo-catalytically degradation of contaminants under Vis irradiation	Electrons in free radicals can be transformed from the valence band to the conduction band under irradiation	[131]

* Degraded or removed; SMX = sulfamethoxazole; CIP = ciprofloxacin; SMT = sulfamethazine; TC = tetracycline; OG = orange; MNZ = metronidazole; # free or surface-bond; KET = ketoprofen; CTC = chloro-tetracycline; SDZ = sulfadiazine; MB = methylene blue; ERF = enrofloxacin (photocatalytic degradation); X-3B = reactive brilliant red X-3B.

For instance, PFRs on BC can activate hydrogen peroxide (H_2O_2) or oxygen (O_2), as well as persulfate ($S_2O_8^{2-}$) to produce different free oxygenated radicals (ROS) capable of efficiently degrade organic contaminants such as chloro-biphenyl [18], phenolic compounds and polychlorinated biphenyls [7], diethyl phthalate [19], thiacloprid [104], and bisphenol A [11]. Moreover, organic chemicals can also be directly degraded on the BC surface by macromolecular free radicals without adding any radical activators [55]. Semiquinone-type radicals present in BC can oxidize As (III) [124]. At the same time, BCs can also exhibit highly effective removal of Cr (VI) by reduction to Cr (III) using PFRs for industrial wastewater remediation [125–129].

Unfortunately, PFRs, by generating surface-bound hydroxyl radicals and free hydroxyl radicals in aqueous solution also in the absence of H_2O_2, can induce various types of cardiovascular and pulmonary disease through ROS-induced oxidative stress (OS) [11]. PFRs and OH radicals detected in the biological fluids generated ROS that induced an oxidant injury and modulated toxic responses in biological tissues [132]. Moreover, quinoid redox cycling is another possible path causing the formation of ROS from material containing semiquinone-type radicals, which could exert toxicity like that exercised by the combustion products present in cigarette smoke [133]. Although BC has beneficial effects on agricultural soil, PFRs in BCs could inhibit plant germination and growth when used in soil remediation. BC addition as a soil amendment has been reported to positively affect plant germination, growth, and yield [134]. In contrast, a negative impact has also been documented when BC-bounded PFRs induce ROS, which can inhibit seed germination and retard growth of root and shoot [18,21]. As shown in Figure 10, the formation and presence of PFRs in the BC produced by several biomasses have been widely documented and studied since 2014.

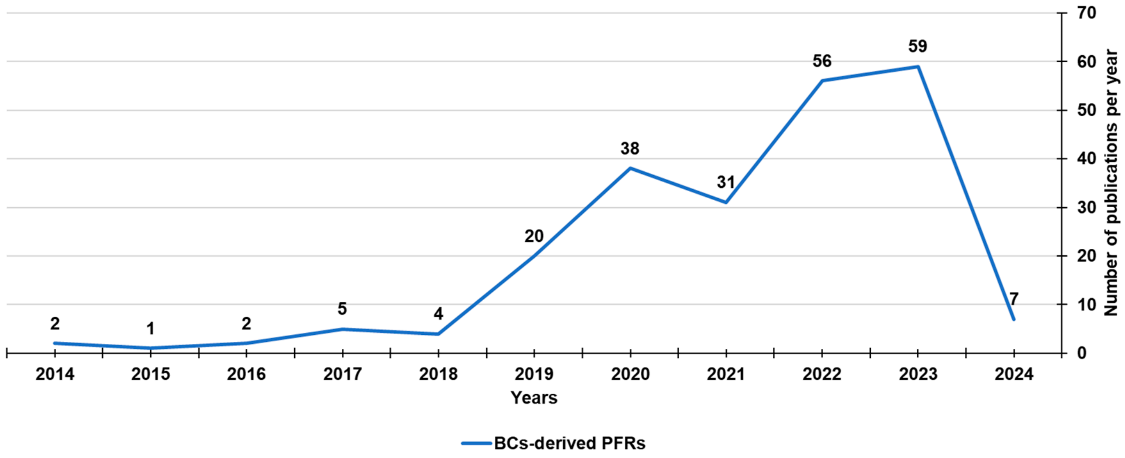

Figure 10. Number of publications on BCs-derived PFRs from 2014 according to Scopus dataset (reviews and chapters in books included). The survey used the following keywords: persistent AND free AND radicals AND biochar.

In this regard, in Table 13, we have reported a random selection of the main experimental works regarding the PFRs found in BCs obtained by different biomasses conveyed in the last five years (2019-2023). Table 13 also summarizes their reported applications including mainly the oxidative degradation of organic environmental pollutants (51 papers), the removal of hazardous inorganic compounds from wastewater such as As (III) and Cr (VI) (12 papers), the degradation of biological samples including bacteria (3 papers), hormones (4 works), genes of bacterial resistance (1 paper), and their use as electrical devices due to their electron and electron donor capacity (EAC and EDC).

Table 13. BC-derived PFRs and their applications as described previously reported in the years 2019-2023.

Biomass	Pyrolysis °C/Time	BC-name	Active radicals	Radical Mechanisms	Application [1] Degraded compound [2]	Refs.
Sawdust	700°C/1h	Fe^0-BC-700	$SO_4^{\bullet -}$ PFRs OH•	Activation of PMS by Fe^0 Activation of PMS by PFRs	BPA [2]	[135]
Waste wood	500°C 700°C	Fe^0-BC	$SO_4^{\bullet -}$ PFRs OH•	Production of PFRs by Fe^0 Activation of PS by Fe^0 Activation of PS by PFRs	TDWW [2]	[136]
Camellia seed husks	400°C/2h	OBC-Fe_3O_4	$SO_4^{\bullet -}$ PFRs OH•	Activation of PS	TC [2]	[137]
Sawdust	300°C 700°C	SBC	$SO_4^{\bullet -}$ PFRs OH•	Activation of PS	AO-7 [2]	[138]
N.R.	200°C 500°C	N.R.	PFRs • O_2^-	UV-induced interaction PFRs/DOM and • O_2^- production	RhB [2]	[139]
Sewage sludge	500°C/4h	HNO_3-BC	PFRs • O_2^- •OH •O_2H	Activation of H_2O_2	CIP [2]	[21]
Wheat straw	500°C/2h	BC/Fe (III)	$SO_4^{\bullet -}$ PFRs OH•	Activation of PS by PFRs	SMX [2]	[140]
Sawdust	700°C	BC700	$SO_4^{\bullet -}$ PFRs OH•	Activation of PDS by PFRs	CA [2]	[141]
Pine needle	500°C/2h	Fe/Mn/BC	•OH	Activation of H_2O_2 by Fe (II), Mn (II) and PFRs (FeMn/BC/H_2O_2 photo-Fenton system)	Naphthalene [2]	[142]
Sewage sludge	500°C/4h	SS-BC	PFRs • O_2^- •OH •O_2H	Activation of O_2 and H_2O_2 by PFRs Degradation of PNP by PFRs	CIP [2]	[143]
Swine manure	600°C	SBC	OCPFRs CCPFRs-O • OH •O_2H	Activation of oxygenated species by OCPFRs and CCPFRs-O (heterogeneous Fenton-like systems SBC/ H_2O_2)	SMT [2]	[144]

Wheat straw	300°C 600°C	BC300 BC600	$\bullet OH$ $\bullet O_2H$	Goethite (Gt)-mediated activation of H_2O_2 (Fenton-like system)	OFX[2]	[145]
Wheat straw	500°C/2h 800°C/2h	CoBCX	$SO_4^{\bullet-}$ PFRs $OH\bullet$	Cobalt and PFRs mediated activation of PMS via O_2	ATZ[2]	[146]
Various crop straws	450, 550 650°C	BC450,550 BC650	$SO_4^{\bullet-}$ $\bullet$ O_2^- $OH\bullet$	BC mediated activation of PS by electron transferring	SDZ[2]	[147]
Tobacco steam	300°C 500°C 700°C	T-BC	ROS	OCPFRs mediated activation of O_2 in the water	PNP[2]	[148]
Pruning wastes of apple trees	400°C550°C 700°C	BC400, BC550 BC700	$SO_4^{\bullet}-$ PFRs	BC and PFRs mediated activation of PS	ACT[2]	[149]
Camphor leaves	400°C/6h	Fe (TPFPP)/BC	$SO_4^{\bullet-}$ PFRs $OH\bullet$	PFRs-mediated electrons transferring to iron porphyrin-loaded BC [3]	PFOA[2]	[150]
Corn stalks	240°C/4h	hydrochar	$\bullet OH$	Electrode and PFRs mediated generation of ROS	2,4-DCP[2]	[151]
Wheat straw	450°C/4h	Co3O4-BC	$SO_4^{\bullet-}$ PFRs $OH\bullet$	Co_3O_4-BCmediated activation of PMS	CAP[2] FF[2] TAP[2]	[152]
Wheat straw Urea Iron salts	800°C/1h	Fe-N-BC	$SO_4^{\bullet-}$ PFRs $\bullet OH$ $\bullet$ O_2^-	Fe, N co-doped BC and PFRs mediated activation of O_2 and PS	AO7[2]	[153]
Candida utilis	700°C/2h	NCS-x	$SO_4^{\bullet-}$ PFRs $OH\bullet$	Activation of PMS by nitrogen-doped biochar nanosheets (NCS-x) using molten salt (NaCl and KCl) in the pyrolysis process	BPA[2] BPF[2] BPS[2] BPAF[2]	[154]
Pine needles	500°C	nFe3O4/BC	PFRs $\bullet O_2H$ $\bullet OH$ $\bullet$ O_2^-	Activation of H_2O_2 by nano-magnetite supported biochar via Fe (III)/Fe (II) cycling and electron transfer with the PFRs	Ethylbenzene[2]	[155]
Sewage sludge	800°C/3h	SM-(0.5:1)	$SO_4^{\bullet-}$ PFRs $OH\bullet$	Activation of PMS by nitrogen-doped sludge biochar with different ratios of melamine in acidic	Cationic/anionic dyes[2]	[156]
Elefant grass	350°C 600°C 900°C 30-120 min	EG	OCPFRs	OCPFRs mediated oxidation	CV[2]	[157]
Sunflower-straw	N.R.	SSBC	$SO_4^{\bullet-}$ PFRs $OH\bullet$	Enhanced Fe (II) activation of PS via BC and PFRs	Benzoic acid[2]	[158]
Pine chips	500°C	OP5 RP5	$SO_4^{\bullet-}$ PFRs $\bullet OH$ $\bullet$ O_2^- $\bullet O_2H$	EDC-involved structures, Fe^{3+} and BC (PFRs) mediated activation of PS in a Fenton-like reaction system using H_2O_2 and NaBH4	2,4-DCP[2]	[159]
Rice straw	350°C 500°C 700°C	BCs MBCs BDOMs	PFRs $\bullet OH$	Direct photocatalytic degradation in BCs and MBCs solutions by Xenon-lamp Oxygen reduction by FPRs of BCs and MBCs BDOMs mediated generation of ROS	SMX[2] CAP[2]	[160]
Pomelo peels	600°C	Fe@PP-Hy-Py	PFRs $\bullet OH$ $\bullet$ O_2^-	Amorphous Fe (0) mediated formation of PFRs Fe (0) mediated reduction of PNP EPFRs mediated oxidation of PNP via ROS (O_2 and H_2O_2) activation	PNP[2]	[161]
Softwood pine	823-873 K	US-BC BC-P BC-P-DEA US-BC-P-DEA US-BC-P-DEA	PFRs $\bullet OH$ $\bullet$ O_2^- $\bullet O_2H$	Reinforcement of PFRs concentration doping BCs with Ni and Pb Activation of H_2O_2 by PFRs	Phenol[2]	[162]
Camphor leaves	500 °C/1h	Fe (VI)/BC-2	Fe(V)/Fe(IV) PFRs $\bullet OH$	Fe (VI)-BC (PFRs) mediated electron transferring and generation of ROS	AZT[2]	[163]
Bagasse powder	800 °C	DBC800 PBC800-A	$SO_4^{\bullet-}$ PFRs $\bullet OH\bullet$ O_2^- $\bullet O_2H$	Enhanced BCs mediated activation of PS Improved PFRs generation by natural endogenous minerals	TC[2]	[164]

Eichhornia crassipes Iron salts	400 °C/2h	MBC	PFRs •OH• O_2^- •O_2H	Fe (II)-BC mediated activation of H_2O_2 (Fenton-like system)	MNZ[2]	[165]
Poplar and pine sawdust	300-500°C	PO xxx PI xxx	SO_4•$^-$ PFRs •OH• O_2^-	Activation of PMS by CCEPFRs-O and CCEPFRs in BC	TC[2] CTC[2] DOX[2]	[166]
S. alfredii	Air-dried	Metal@P	•O_2H	PFRs generation by the thermochemical behaviour of Mn and Zn Electron transfer Activation of PDS by PFRs in Fe/Zn@PB9/PDS system AOPs	Imidacloprid[2]	[167]
Sludge	N.R.	N.R.	SO_4•$^-$ PFRs •OH• O_2^-	Production of ROS via PFRs Mn-mediated electron transfer through Mn-doped sludge-based biochar (BC) mediated the	CIP[2]	[168]
Cellulose Lignin	200-1000°C	C200, C500 C1000 L200, L500 L1000	SO_4•$^-$PFRs • O_2^-	Activation of PS adsorbed onto BCs via PFRs, oxygen-containing functional groups, and defective structures of BCs	OFX[2]	[169]
Chestnut shell $KMnO_4$	700 °C/1h 400 °C/1h	Mn-BC	PFRs	Mn-improved electron-transfer	OTC[2]	[170]
Spent coffee TiO_2	300 °C 500 °C 600 °C	SBC500	PFRs •OH• O_2^- •O_2H	Activation of H_2O_2 by Ti-doped H_2SO_4-modified biochar (SBCs) (Photo-Fenton-like system)	MO[2]	[171]
RS	550 °C/2h	BC-α-Fe2O3/MgO	PFRs •OH• O_2^- •O_2H	UV light activation of PFRs Production of O_2 upon NPA degradation O_2 activation by PFRs	NPA[2]	[172]
Sewage sludge	400 °C/2h	SDBC	PFRs •OH• O_2^- •O_2H	O_2 activation by PFRs promoted by HNO_3 or NaOH environmental	*p*-Chlorophenol[2]	[173]
Peanut hull	700 °C/2h	BC-Fe-1-Zn	SO_4•$^-$ PFRs •OH	Activation of PS by bimetal-modified peanut hull-derived biochar via Fe and Zn oxides and oxygen-containing functional groups active sites	TC[2]	[174]
Blue algae	700 °C	Z-700 FeOX@BC	SO_4•$^-$ PFRs •OH •O_2^-•O_2H	• O_2^- production by FeOX (zero-valent iron and iron oxide) C=C, C=O, O-C=O, Fe-O functional groups and PFRs promoted the activation of PDS	TC[2]	[175]
Biomasses	300-1000 °C	N.R.	SO_4•$^-$ PFRs •OH • O_2^-	Activation of PS and PMS by physical and chemical modified BCs using acid/alkali treatment and metal doping via PFRs	PPCPs[2]	[176]
Chicken feathers	350°C/4h 800°C/4h	MBC35@FH MBC80@FH	SO_4•$^-$ PFRs •OH • O_2^-	Activation of PDS by the transformation of Fe species, oxygen-containing functional groups, pyrrolic nitrogen, and PFRs to produce ROS	TPhP[2]	[177]
Pine needles	300-900 °C	BC300-900	SO_4•$^-$ PFRs •OH • O_2^-	Activation of PMS by BC via ROS production or electron transfer capability	OFX[2] ENR[2] FLE[2]	[178]
PolyS	220°C/2h $^{\$}$ 500°C /2h $^{\#}$ 900°C /2h $^{\#}$	BC500 + PS BC900 + PS BC500 BC900	SO_4•$^-$ PFRs •OH • O_2^-	Activation of PMS using CCEPFRs on BC-aged by microbial fermentation for ROS production	SDZ[2] OFX[2] DOX[2]	[179]
Red mud Wheat crop	700°C /2h	MRBC	SO_4•$^-$PFRs • OH	PDS activation by the active sites of MRBC, such as Fe (II) and PFRs	LFX[2]	[180]
Various sludges	300-900°C 2h	S-HPBC S-PBC S-HBC	SO_4•$^-$ PFRs •OH • O_2^-	Activation of PS by PFRs mediated electrons transferring activity Electrons transferring to Cr (VI) by PFRs	TC[2] Cr (VI) ⇒ Cr (III) [1]	[181]
Peanut shells	500 °C/4 h	BC-Ce	OFGs, CCPFRs	Electrons transferring to Cr (VI) by OFGs, CCPFRs, oxygen vacancies and graphitic structure in BC-Ce promoted by CeO_2	Cr (VI) ⇒ Cr (III) [1]	[182]
Rice husk	400°C/1h	BC400	OH• H_2O_2	(pH acid) Activation of O_2 by phenol OH and semiquinone types PFRs	As (III) ⇒ As (V) [1]	[124]

			Semiquinone-type PFRs Quinoid C═O H_2O_2	(pH alkaline) Activation of O_2 by phenol OH and semiquinone types PFRs		
Rice husk	550°C	RH-BC	PRFs	Promotion of OCPFRs by BC-inducted Cr (VI) degradation	Cr (VI) ⇒ Cr (III) ^{1}	[125]
Stalk	450°C/90 min	NBC	PFRs	N-doped BC mediated evolution of PFRs for the transformation of Cr (VI)	Cr (VI) ⇒ Cr (III) ^{1}	[126]
Rice husk	500°C/2h	MGBs	PFRs •OH • O_2^-	Efficient surface Fe (III)/Fe (II) cycling via electron transfer with the PFRs of magnetic greigite/BC composites (MGBs)	Cr (VI) ⇒ Cr (III) ^{1}	[127]
Sludge	220 °C/2h	BC	OCPFRs	UV-Vis photo-irradiation enhanced the production of PFRs Action of OCPFRs as electron donors to transform Cr (VI) into Cr (III)	Cr (VI) ⇒ Cr (III) ^{1}	[128]
Sludge	120 °C	SBC120	OCPFRs	OCPFRs mediated electrons transferring to Cr (VI) in neutral solutions	Cr (VI) ⇒ Cr (III) ^{1}	[129]
	270 °C	SBC270	CCPFRs	CCPFRs mediated electrons transferring to Cr (VI) in neutral solutions		
Rice husk	400°C/1h	rUBC, rDBC	Quinoid C=O PFRs	Quinoid C=O and PFRs mediated oxidation of As (III)	As (III) ⇒ As (V) ^{1}	[183]
Maize straw powder	500°C/2h	FhBC	PFRs • O_2^- •OH	Fe and PFRs mediated activation of O^2 and H_2O_2	As (III) ⇒ As (V)^{1}	[184]
Sewage sludge	270 °C/2h	SBC	$SO_4^{\bullet -}$ PFRs •OH • O_2^-	Activation of PS by SBC via PFRs mediated electrons transferring	As (III) ⇒ As (V) ^{1}	[185]
Pinewood	600°C/1h	Fe/HC	• O_2^- •OH	Activation of O_2 and H_2O_2 by CCPFRs	Estrogens ^{2}	[186]
Rice straw	500°C/1h	BiPB	•OH PFRs	Generation of •OH by Bi/Bi_2O_3 and PFRs	Estrone ^{2,*}	[187]
Anaerobic digestion sludge	400°C 600°C 800°C 1000°C	ADSBC 400 ADSBC 600 ADSBC 800 ADSBC 1000	$SO_4^{\bullet -}$ PFRs OH•	BC-mediated activation of PDS	Dyes^{2} Estrogens^{2} Sulfonamides^{2} *E. coli*^{2} Others^{2}	[188]
Walnut shell	700 °C/1h	BC700	PFRs	Oxidation by PFRs-mediated electron transfer	E1^{2} E2^{2} E3^{2}	[189]
Caragana korshinskii	650 °C/3h	ACB-K-gC3N	PFRs h^+•OH• O_2^-	Electron photogeneration and PFRs mediated H_2O and O_2 activation	*S. aureus*^{2} *E. coli*^{2} RhB^{2} TA^{2} NOR^{2} CAP^{2}	[190]
Pinewood	600°C	Ag^0-PBC	PFRs •OH • O_2^-	UV-light promoted excitation of the electron-hole pairs and Subsequently, the production of ROS Enhanced ROS generation by PFRs	MB^{2} *E. coli*^{2}	[191]
Rice straw	400°C 700°C 120 min	Nano-BC	PFRs •OH • O_2^-	Oxidation and damage by ROS	eDNA^{2}	[192]
Rice straw	500°C	RS-BC	Quinones Phenols PFRs	By electron acceptor capacity (EAC) By electron donor capacity (EDC)	⇆ Redox property ^{1} Electronic storage ^{1}	[193]

BCs = biochar; MBCs = modified-biochar; BDOMs = biochar-derived dissolved organic matters; PMS = peroxy-mono-sulfate; BPA = bisphenol A; PS = persulfate; TDWW = textile dyeing wastewater; TC = tetracycline; (TDWW); SBC = sawdust biochar; AO-7 = acid orange 7; RhB = rhodamine B; DOM = dissolved organic matter in BC; CIP = ciprofloxacin; SMX = sulfamethoxazole; PDS = peroxydisulfate; CA = clofibric acid; WW = wastewater; ⇆ = reversible; PNP = p-nitrophenol (water pollutant); SMT = sulfamethazine; SDZ = sulfadiazine; OCPFRs = oxygen-centered environmental persistent free radicals; CCPFRs-O = carbon-centered environmental persistent free radicals with oxygen atoms; * photocatalytic; CCPFRs = carbon-centered environmental persistent free radicals; BiPB = bismuth-containing BC; PFX = pefloxacin; OTC = oxytetracycline; CTC = chlorotetracycline; OFX = ofloxacin; AZT = atrazine; TMP = trimethoprim; AOPs = advanced oxidation processes; ACT = acetaminophen; PFOA = perfluorooctanoic acid; 3 degradation efficiency in presence of ascorbic acid (AA); 2,4-DCP = 2,4-dichlorophenol; CAP = chloramphenicol; FF = florfenicol; TAP = thiamphenicol; CV = crystal violet dye; MB = methylene blue; MNZ = metronidazole; DOX = doxorubicin; xxx = refers to the temperature of pyrolysis process; NPA = N-phosphono methyl iminodiacetic acid (organophosphorus pesticide (OP); NOR = norfloxacin; E1 = estrone; E2 = 17-estradiol; E3 = estriol; PPCPs = pharmaceuticals and personal care products; TPhP = triphenyl phosphate; ENR = enrofloxacin; FLE = fleroxacin (FLE); $ HTC = hydro-thermal carbonization;

HTP = high temperature pyrolysis; PolyS = polystyrene; OFGs = oxygen-containing functional group; S-HPBC = S-doped hydrothermal + pyrocarbon BC; S-HBC = S-doped hydrochar, S-PBC = S-doped pyrocarbon. Figure 11 shows the relative abundances of the types of PFRs applications concerning the 72 case studies considered here.

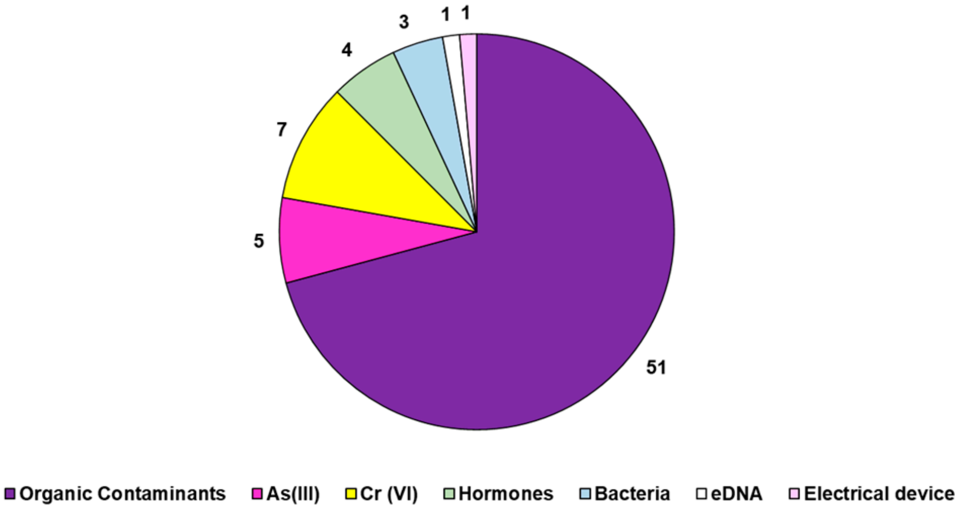

Figure 11. Number of publications for each type of EPRs application found in literature considering a randomly selected population of 72 papers published in 2019-2023.

As for the mechanisms, many publications regarded the activation, sometimes photocatalytic, of PS, PMS, and PDS by BC. The employed BC was derived from different feedstock biomasses (bagasse powder, poplar, and pine sawdust, cellulose, lignin, Blue algae, waste straw, and other sources as reported in Table13), not doped or doped with nitrogen atoms or different metals including Fe, Mn, Co, Ni, Zn. In these processes, the electron transfer promoted by metals and/or PFRs of diverse nature, based on the pyrolysis conditions, generated ROS such as $SO_4•^-$, •OH, $•O_2^-$, $•O_2H$ and non-radical species ($^1O_2$), which carried out the oxidative degradation of different organic xenobiotics, including drugs, dyes, antibiotics, hormones, as well as phenols or aromatic derivatives. Many other publications reported the use of BC to activate or photochemically activate O_2 or H_2O_2 (Fenton-like systems) via metal and/or PFRs-mediated single electron transfer. The generated ROS (•OH, $•O_2^-$, $•O_2H$) and oxygen non-radical species ($^1O_2$) successfully oxidized several organic pollutants, degraded hormones and eDNA and, in some cases, showed antibacterial effects against *E. coli* and *S. aureus*. Moreover, the capacity of BC to transfer electrons via transitional metals or PFRs was used to oxidize As (III) to As (V) or reduce Cr (VI) to Cr (III), thus resulting in helping to remove hazardous inorganic contaminants from industrial wastewater.

3.2.2. BC-Associated PFRs Shadows: Cytotoxicity and Biotoxicity

Despite the plethora of possible beneficial applications of BC, PFRs, as well as other free radicals and toxic substances that compose it, such as heavy metals, PAHs, dioxins, and perfluorochemicals (PFCs), are released into the environment during the pyrolysis process, thus representing a potential risk to the environment and humans [194]. Additionally, as well as other contaminants, the possible carbon allotropes forming during pyrolysis are severe contaminants in air, water, and soil [195]. Black carbon, carbon black (CB), carbon nanotubes, graphene, quantum dots, and fullerenes can possess distinct toxicity depending on many factors, including type of allotrope, particle size, form, structural defects, coating molecules, grade of functionalization [195]. Understanding the toxicity of such carbon nanomaterials and nanoproducts possibly present in BC is essential for human and environmental health, safety, and public acceptance. In this regard, recent studies have focused their attention on the adverse effects of BC due to its particle size and the various interactions with the environment that could occur [196,197]. Upon its application, BC may produce harmful environmental effects due to aging by oxidative or biological processes leading to changes in its properties [198,199]. Additionally, higher toxicity has been reported for BC with micro or nano dimensioned particles. It has been reported that the presence of micro-BC (MBC) or nano-BC (NBC) can promote the release of heavy metal ions into the medium when applied to soil [194]. Kim et al. (2018) observed that BC particles with a particle size of less than 0.45 μm could increase the release and mobility of As in soil [200]. Regarding the biotoxicity of MBC/NBC, it has been previously reported that particle-induced oxidative stress is a crucial mechanism of MBC/NBC cytotoxicity, which increases as the particle size decreases. Also, the PFRs concentration on the surface of particles with an aerodynamic diameter of less than 1 μm is the highest [121,201]. While, several reviews and studies exist on the production and modification of BC, the reaction mechanisms, and the beneficial active role of BC in environmental remediation, the adverse effects and potential risks of BC have only recently been evidenced. The comprehensive phenomena and mechanisms involved in BC toxicity still require elucidation, especially in environmental media different from soil, including water and the atmosphere. It is imperative to systematically study and discuss the possible adverse environmental effects of BC application concerning various media, including water and atmosphere, by determining the corresponding occurrence, detection, assessment, and avoidance measures. Worryingly, the current knowledge concerning the possible adverse effects on the environment and biota deriving from the extensive application of PFRs originating in BC is even more limited [202]. Although they are emerging as contaminants of increasing concern, their formation, fate, toxicity, and health risks are poorly known [202]. Thermal treatment, a common remediation technique to clean industrial soils, induces the formation of PFRs, which could paradoxically increase soil toxicity, contrary to the original remediation objective. For example, there is still little knowledge on the formation and toxicity of PFRs in soils contaminated by polycyclic aromatic hydrocarbons (PAHs) [203]. BC-derived PFRs, as well as those present in the environment and deriving from combustion and soil restoration, the burning of coal, wood, straw, cigarettes, oil, and other fuels, and from the restoration of organic contaminated soil, can enter the human body mainly through three pathways including respiratory tract, skin exposure and ingestion [132]. PFRs are not toxic to living beings and the environment, but they can stimulate the formation of other harmful substances and free radicals, including various types of ROS, when in the environment or in vivo [203]. As well documented, ROS can interfere with the normal redox and metabolic processes, thus causing oxidative stress in biota [204]. Additionally, it has been reported that exposure to PFRs may induce cell degeneration or apoptosis and may affect the normal functions of the heart or lungs of humans [203]. So far, cytotoxicity and biotoxicity are the two categories of toxicity reported as attributable to PFRs (Table 14).

Table 14. Potential toxic hazards caused by PFR exposure.

Target	Danger	Material source	Refs.
Cells	⇑ Lungs' T (Th1, Th2, Th17) cells	PM, DCB230, MCP230	[205,206]
	⇓ P450 activity	PM, MCP230	[207]
	Cardiomyocytes' apoptosis	DCB230	[208]
	⇓ Survival of gastric epithelial cells	BaP–Na montmorillonite	[209]
	Loss of normal morphology of pulmonary epithelial cells	DCB230	[210]
	Mitochondrial depolarization	DCB230	[206]
	Changes in VEGF	ZnO/MCB	[211]

Target	Danger	Material source	Refs.
Enzymes Proteins Genes	Altered expression activity of Cyp1a, Cyp2b, Cyp2e1, Cyp2d2, Cyp3a and other genes	DCB230, MCP230	[205]
	⇑ Expression levels of peroxiredoxin-6 Cofilin 1, annexin A8	MCP230, CGUFP, ZnO/MCB	[206]
	⇓ of GSH, GPx, SOD	ZnO/MCB	[212]
Organs and tissues	Altered normal renal hemodynamics and urodynamics	N.R.	[213]
	Liver damage	N.R.	[214]
	Impair left ventricular function	DCB230	[215]
	Airway hyperresponsiveness Lung inflammation	MCP230	[216]
Individuals	Abnormalities in zebrafish	DCB230	[217]
	⇓ Growth and reproduction of luminescent bacteria	PM	[218]
	Altered behavior of *Caenorhabditis elegans*	Biochar	[219]
	⇓ Energy consumption	MCP230	[220]
Disease	⇑ Severity of the flu	DCB230	[221]
	Asthma	MCP230	[206]
	Cardiovascular disease and dysfunction	DCB230	[208]
Other damage	Oxidative stress	DCB230, ZnO/MCB	[212]
	DNA damage	BaP	[222]
	Lipid peroxidation	MCP230	[223]

⇑ Improved, increased; ⇓ decreased, inhibited; PM = particulate matter; DCP230 = 1,2-dichlorobenzene at 230 ◦C; MCP230 = mono-chlorophenol at 230 ◦C; MCB = mono-chlorobenzene; CGUFP = combustion generated ultrafine particle; N.R. = not reported; GSH = glutathione; GPx = glutathione. Peroxidase; SOD = superoxide dismutase; VEGF = vascular endothelial growth factor.

Usually, toxicity tests are carried out in research laboratories using both environmental samples and lab-prepared PFRs, such as those generated by MCP230 (a mixture of CuO and chlorophenol at 230 ◦C), DCB230 (a mixture of CuO, 0.2 µm amorphous silica and 1,2-dichlorobenzene at 230 ◦C), CGUFP (combustion generated ultrafine particle) or other mixtures of transitional metals and substituted aromatic compounds. For cytotoxicity experiments, cultured cells extracted from the bronchial epithelium and rats are used, while biotoxicity essays are carried out on plants, fishes, rabbits, and worms. Generally, it was observed that exposure to PFRs causes oxidative stress. More specifically, cytotoxicity tests evidenced cell variation, decreased number and activity, the disparity in protein expression, and DNA damage. Biotoxicity experiments revealed abnormalities in development and behaviour, disease, and organ and tissue damage. Although BC can serve as an environmentally sustainable soil amendment due to its ability to enhance several chemical properties of soil, such as pH, electrical conductivity, CEC, and organic carbon content, thus contributing to the overall improvement of nutrient retention in the soil, BC with high concentrations of PFRs negatively affect crop growth.

Additionally, it has been found that PFRs in the aquicultural solution inhibited the germination rate of different crops by ROS induction [132]. The oxidative stress brought by the production of ROS can also damage the plasma membrane of the root system and hinder plant root growth. Moreover, PFRs induced neurotoxicity of *Cryptobacterium hidradenoma*, transforming it into a neurotoxin for soil organisms and posing a threat to their survival.

4. Risk Prevention Strategies and Conclusions

This review has evidenced that BC and mainly PFRs, generated during the pyrolysis processes performed to produce it could be double-edged weapons. BC is reported to be an eco-friendly and low-cost black gold with many beneficial properties, including the capability to remove organic and inorganic pollutants from water by adsorption processes and/or through its PFRs. Anyway, several studies have reported that PFRs can be very dangerous to the environment and humans by a ROS-dependent mechanism. In addition to being produced by various common xenobiotics, PFRs can be easily converted into secondary pollutants, causing further biotoxicity. The still too little studied transport and transformation of PFRs in the environment can also affect the behavior of other substances, leading to potential environmental hazards that are not yet fully understood. Therefore, the further exploration of the ecological impact of PFRs and the development of prevention and control measures are necessary. In this regard, although some progress has been made in the environmental risk and biotoxicity studies concerning PFRs, research is still in the initial stage, and there is an urgent need for systematic and in-depth studies on the production and transport of PFRs. A more in-depth understanding of the influence of the environmental conditions on their occurrence is needed to control the external factors for reducing the output of PFRs and promoting the degradation of xenobiotics. A more rational knowledge about their toxicity mechanisms is necessary to have a more precise toxicological equivalence regulation. A better strategy to prevent the risks associated with PFRs is avoiding exposure to them by reducing contact with combustion sources, such as vehicle exhaust and cigarette smoke. Proper air filtration systems removing PFRs from indoor air and tearing protective masks or respirators can lower the possibility of contact with PFRs in outdoor environments. Additionally, treatments for limiting the adverse health effects associated with PFRs exposure, such as using antioxidants, which can neutralize ROS, could be another strategy to protect humans from the adverse impacts of PFR exposure.

Author Contributions: The authors (S.A. and O.G.P.) contributed equally to this work.

Funding: This research received no external funding.

Institutional Review Board Statement: Not applicable.

Informed Consent Statement: Not applicable.

Conflicts of Interest: The authors declare no conflict of interest.

References

1. Zhang, R.; Zhang, R.; Zimmerman, A.R.; Wang, H.; Gao, B. Applications, Impacts, and Management of Biochar Persistent Free Radicals: A Review. *Environmental Pollution* **2023**, *327*, 121543, doi:10.1016/j.envpol.2023.121543.
2. Wang, J.; Wang, S. Preparation, Modification, and Environmental Application of Biochar: A Review. *Journal of Cleaner Production* **2019**, *227*, 1002–1022, doi:10.1016/j.jclepro.2019.04.282.
3. Premarathna, K.S.D.; Rajapaksha, A.U.; Sarkar, B.; Kwon, E.E.; Bhatnagar, A.; Ok, Y.S.; Vithanage, M. Biochar-Based Engineered Composites for Sorptive Decontamination of Water: A Review. *Chemical Engineering Journal* **2019**, *372*, 536–550, doi:10.1016/j.cej.2019.04.097.
4. Beesley, L.; Moreno-Jiménez, E.; Gomez-Eyles, J.L.; Harris, E.; Robinson, B.; Sizmur, T. A Review of Biochars' Potential Role in the Remediation, Revegetation and Restoration of Contaminated Soils. *Environmental Pollution* **2011**, *159*, 3269–3282, doi:10.1016/j.envpol.2011.07.023.

5. Jeffery, S.; Verheijen, F.G.A.; van der Velde, M.; Bastos, A.C. A Quantitative Review of the Effects of Biochar Application to Soils on Crop Productivity Using Meta-Analysis. *Agriculture, Ecosystems & Environment* **2011**, *144*, 175–187, doi:10.1016/j.agee.2011.08.015.
6. Kinney, T.J.; Masiello, C.A.; Dugan, B.; Hockaday, W.C.; Dean, M.R.; Zygourakis, K.; Barnes, R.T. Hydrologic Properties of Biochars Produced at Different Temperatures. *Biomass and Bioenergy* **2012**, *41*, 34–43, doi:10.1016/j.biombioe.2012.01.033.
7. Qin, Y.; Li, G.; Gao, Y.; Zhang, L.; Ok, Y.S.; An, T. Persistent Free Radicals in Carbon-Based Materials on Transformation of Refractory Organic Contaminants (ROCs) in Water: A Critical Review. *Water Research* **2018**, *137*, 130–143, doi:10.1016/j.watres.2018.03.012.
8. Vejerano, E.P.; Rao, G.; Khachatryan, L.; Cormier, S.A.; Lomnicki, S. Environmentally Persistent Free Radicals: Insights on a New Class of Pollutants. *Environ. Sci. Technol.* **2018**, *52*, 2468–2481, doi:10.1021/acs.est.7b04439.
9. Volpe, R.; Bermudez Menendez, J.M.; Ramirez Reina, T.; Volpe, M.; Messineo, A.; Millan, M.; Titirici, M.-M. Free Radicals Formation on Thermally Decomposed Biomass. *Fuel* **2019**, *255*, 115802, doi:10.1016/j.fuel.2019.115802.
10. Huang, Y.; Guo, X.; Ding, Z.; Chen, Y.; Hu, X. Environmentally Persistent Free Radicals in Biochar Derived from Laminaria Japonica Grown in Different Habitats. *Journal of Analytical and Applied Pyrolysis* **2020**, *151*, 104941, doi:10.1016/j.jaap.2020.104941.
11. Ruan, X.; Sun, Y.; Du, W.; Tang, Y.; Liu, Q.; Zhang, Z.; Doherty, W.; Frost, R.L.; Qian, G.; Tsang, D.C.W. Formation, Characteristics, and Applications of Environmentally Persistent Free Radicals in Biochars: A Review. *Bioresource Technology* **2019**, *281*, 457–468, doi:10.1016/j.biortech.2019.02.105.
12. Wang, R.-Z.; Huang, D.-L.; Liu, Y.-G.; Zhang, C.; Lai, C.; Wang, X.; Zeng, G.-M.; Gong, X.-M.; Duan, A.; Zhang, Q.; et al. Recent Advances in Biochar-Based Catalysts: Properties, Applications and Mechanisms for Pollution Remediation. *Chemical Engineering Journal* **2019**, *371*, 380–403, doi:10.1016/j.cej.2019.04.071.
13. Odinga, E.S.; Waigi, M.G.; Gudda, F.O.; Wang, J.; Yang, B.; Hu, X.; Li, S.; Gao, Y. Occurrence, Formation, Environmental Fate and Risks of Environmentally Persistent Free Radicals in Biochars. *Environment International* **2020**, *134*, 105172, doi:10.1016/j.envint.2019.105172.
14. Fang, G.; Liu, C.; Gao, J.; Dionysiou, D.D.; Zhou, D. Manipulation of Persistent Free Radicals in Biochar To Activate Persulfate for Contaminant Degradation. *Environ. Sci. Technol.* **2015**, *49*, 5645–5653, doi:10.1021/es5061512.
15. He, J.; Xiao, Y.; Tang, J.; Chen, H.; Sun, H. Persulfate Activation with Sawdust Biochar in Aqueous Solution by Enhanced Electron Donor-Transfer Effect. *Science of The Total Environment* **2019**, *690*, 768–777, doi:10.1016/j.scitotenv.2019.07.043.
16. Wang, H.Z.; Guo, W.Q.; Yin, R.L.; Du, J.S.; Wu, Q.L.; Luo, H.C.; Liu, B.H.; Sseguya, F.; Ren, N.Q. Biochar-induced Fe(III) reduction for persulfate activation in sulfamethoxazole degradation: insight into the electron transfer, radical oxidation and degradation pathways. *Chem. Eng. J.* **2019**, *362*, 561-569.
17. Liang, J.; Xu, X.; Qamar Zaman, W.; Hu, X.; Zhao, L.; Qiu, H.; Cao, X. Different Mechanisms between Biochar and Activated Carbon for the Persulfate Catalytic Degradation of Sulfamethoxazole: Roles of Radicals in Solution or Solid Phase. *Chemical Engineering Journal* **2019**, *375*, 121908, doi:10.1016/j.cej.2019.121908.
18. Fang, G.; Gao, J.; Liu, C.; Dionysiou, D.D.; Wang, Y.; Zhou, D. Key Role of Persistent Free Radicals in Hydrogen Peroxide Activation by Biochar: Implications to Organic Contaminant Degradation. *Environ. Sci. Technol.* **2014**, *48*, 1902–1910, doi:10.1021/es4048126.
19. Fang, G.; Zhu, C.; Dionysiou, D.D.; Gao, J.; Zhou, D. Mechanism of Hydroxyl Radical Generation from Biochar Suspensions: Implications to Diethyl Phthalate Degradation. *Bioresource Technology* **2015**, *176*, 210–217, doi:10.1016/j.biortech.2014.11.032.
20. Fang, G.; Liu, C.; Wang, Y.; Dionysiou, D.D.; Zhou, D. Photogeneration of Reactive Oxygen Species from Biochar Suspension for Diethyl Phthalate Degradation. *Applied Catalysis B: Environmental* **2017**, *214*, 34–45, doi:10.1016/j.apcatb.2017.05.036.
21. Luo, K.; Yang, Q.; Pang, Y.; Wang, D.; Li, X.; Lei, M.; Huang, Q. Unveiling the Mechanism of Biochar-Activated Hydrogen Peroxide on the Degradation of Ciprofloxacin. *Chemical Engineering Journal* **2019**, *374*, 520–530, doi:10.1016/j.cej.2019.05.204.
22. Zhang, Y.; Xu, M.; He, R.; Zhao, J.; Kang, W.; Lv, J. Effect of Pyrolysis Temperature on the Activated Permonosulfate Degradation of Antibiotics in Nitrogen and Sulfur-Doping Biochar: Key Role of

Environmentally Persistent Free Radicals. *Chemosphere* **2022**, *294*, 133737, doi:10.1016/j.chemosphere.2022.133737.

23. Liao, S.; Pan, B.; Li, H.; Zhang, D.; Xing, B. Detecting Free Radicals in Biochars and Determining Their Ability to Inhibit the Germination and Growth of Corn, Wheat and Rice Seedlings. *Environ. Sci. Technol.* **2014**, *48*, 8581–8587, doi:10.1021/es404250a.
24. Ahmad, M.; Rajapaksha, A.U.; Lim, J.E.; Zhang, M.; Bolan, N.; Mohan, D.; Vithanage, M.; Lee, S.S.; Ok, Y.S. Biochar as a Sorbent for Contaminant Management in Soil and Water: A Review. *Chemosphere* **2014**, *99*, 19–33, doi:10.1016/j.chemosphere.2013.10.071.
25. Qin, J.; Chen, Q.; Sun, M.; Sun, P.; Shen, G. Pyrolysis Temperature-Induced Changes in the Catalytic Characteristics of Rice Husk-Derived Biochar during 1,3-Dichloropropene Degradation. *Chemical Engineering Journal* **2017**, *330*, 804–812, doi:10.1016/j.cej.2017.08.013.
26. Yang, J.; Pignatello, J.J.; Pan, B.; Xing, B. Degradation of P-Nitrophenol by Lignin and Cellulose Chars: H2O2-Mediated Reaction and Direct Reaction with the Char. *Environ. Sci. Technol.* **2017**, *51*, 8972–8980, doi:10.1021/acs.est.7b01087.
27. Ginoble Pandoli, O.; Santos de Sá, D.; Nogueira Barbosa Junior, M.; Paciornik, S. Bamboo-Based Lignocellulose Biomass as Catalytic Support for Organic Synthesis and Water Treatments. In: Palombini, F.L.; Nogueira, F.M. (eds) *Bamboo Science and Technology. Environmental Footprints and Eco-design of Products and Processes*. 2023, Springer, Singapore, pp. 297-327. https://doi.org/10.1007/978-981-99-0015-2_11.
28. Jahirul, M.I.; Rasul, M.G.; Chowdhury, A.A.; Ashwath, N. Biofuels Production through Biomass Pyrolysis —A Technological Review. *Energies* **2012**, *5*, 4952–5001, doi:10.3390/en5124952.
29. Yaashikaa, P.R.; Senthil Kumar, P.; Varjani, S.J.; Saravanan, A. A Review on Photochemical, Biochemical and Electrochemical Transformation of CO2 into Value-Added Products. *Journal of CO2 Utilization* **2019**, *33*, 131–147, doi:10.1016/j.jcou.2019.05.017.
30. Saidur, R.; Abdelaziz, E.A.; Demirbas, A.; Hossain, M.S.; Mekhilef, S. A Review on Biomass as a Fuel for Boilers. *Renewable and Sustainable Energy Reviews* **2011**, *15*, 2262–2289, doi:10.1016/j.rser.2011.02.015.
31. Yaashikaa, P.R.; Kumar, P.S.; Varjani, S.; Saravanan, A. A Critical Review on the Biochar Production Techniques, Characterization, Stability and Applications for Circular Bioeconomy. *Biotechnology Reports* **2020**, *28*, e00570, doi:10.1016/j.btre.2020.e00570.
32. Lehmann, J. Biochar for environmental management: an introduction. Biochar for Environmental Management. *Sci. Technol.* **2009**, *25*, 15801-15811.
33. Mohanty, S.K.; Valenca, R.; Berger, A.W.; Yu, I.K.M.; Xiong, X.; Saunders, T.M.; Tsang, D.C.W. Plenty of Room for Carbon on the Ground: Potential Applications of Biochar for Stormwater Treatment. *Science of The Total Environment* **2018**, *625*, 1644–1658, doi:10.1016/j.scitotenv.2018.01.037.
34. Ayla Norris Smidth. A New Boost for Biochar as a Natural Climate Solution. 2023. Available online at https://blog.nature.org/science-brief/a-new-boost-for-biochar-as-a-natural-climate-solution/#:~:text=Biochar%20is%20a%20type%20of%20charcoal%20made%20from,other%20biomass%20would%2C%20leading%20to%20more%20carbon%20sequestration (accessed on December 27, 2023).
35. Yu, D.; Yu, Y.; Tang, J.; Li, X.; Ke, C.; Yao, Z. Application Fields of Kitchen Waste Biochar and Its Prospects as Catalytic Material: A Review. *Science of The Total Environment* **2022**, *810*, 152171, doi:10.1016/j.scitotenv.2021.152171.
36. Yu, S.; Zhang, W.; Dong, X.; Wang, F.; Yang, W.; Liu, C.; Chen, D. A Review on Recent Advances of Biochar from Agricultural and Forestry Wastes: Preparation, Modification and Applications in Wastewater Treatment. *Journal of Environmental Chemical Engineering* **2024**, *12*, 111638, doi:10.1016/j.jece.2023.111638.
37. Wijitkosum, S. Biochar Derived from Agricultural Wastes and Wood Residues for Sustainable Agricultural and Environmental Applications. *International Soil and Water Conservation Research* **2022**, *10*, 335–341, doi:10.1016/j.iswcr.2021.09.006.
38. Yao, Y.; Gao, B.; Inyang, M.; Zimmerman, A.R.; Cao, X.; Pullammanappallil, P.; Yang, L. Biochar Derived from Anaerobically Digested Sugar Beet Tailings: Characterization and Phosphate Removal Potential. *Bioresource Technology* **2011**, *102*, 6273–6278, doi:10.1016/j.biortech.2011.03.006.
39. Puettmann, M.; Sahoo, K.; Wilson, K.; Oneil, E. Life Cycle Assessment of Biochar Produced from Forest Residues Using Portable Systems. *Journal of Cleaner Production* **2020**, *250*, 119564, doi:10.1016/j.jclepro.2019.119564.

40. Papageorgiou, A.; Azzi, E.S.; Enell, A.; Sundberg, C. Biochar Produced from Wood Waste for Soil Remediation in Sweden: Carbon Sequestration and Other Environmental Impacts. *Science of The Total Environment* **2021**, *776*, 145953, doi:10.1016/j.scitotenv.2021.145953.
41. Laird, D. Biochar Amendments Make the Harvesting of Crop Residue for Bioenergy Production Sustainable. *Nutrient Cycling in Agroecosystems* **2023**, doi:10.1007/s10705-023-10281-1.
42. Li, N.; He, M.; Lu, X.; Yan, B.; Duan, X.; Chen, G.; Wang, S.; Hou, L. Municipal Solid Waste Derived Biochars for Wastewater Treatment: Production, Properties and Applications. *Resources, Conservation and Recycling* **2022**, *177*, 106003, doi:10.1016/j.resconrec.2021.106003.
43. Shi, W.; Wang, H.; Yan, J.; Shan, L.; Quan, G.; Pan, X.; Cui, L. Wheat Straw Derived Biochar with Hierarchically Porous Structure for Bisphenol A Removal: Preparation, Characterization, and Adsorption Properties. *Separation and Purification Technology* **2022**, *289*, 120796, doi:10.1016/j.seppur.2022.120796.
44. Foong, S.Y.; Chan, Y.H.; Chin, B.L.F.; Lock, S.S.M.; Yee, C.Y.; Yiin, C.L.; Peng, W.; Lam, S.S. Production of Biochar from Rice Straw and Its Application for Wastewater Remediation − An Overview. *Bioresource Technology* **2022**, *360*, 127588, doi:10.1016/j.biortech.2022.127588.
45. Gunamantha, M.; Widana, G.A.B. *IOP Conf. Ser.: Earth Environ. Sci.* **2018**, 131 012055.
46. Rathnayake, D.; Schmidt, H.-P.; Leifeld, J.; Mayer, J.; Epper, C.A.; Bucheli, T.D.; Hagemann, N. Biochar from Animal Manure: A Critical Assessment on Technical Feasibility, Economic Viability, and Ecological Impact. *GCB Bioenergy* **2023**, *15*, 1078–1104, doi:10.1111/gcbb.13082.
47. Drané, M.; Zbair, M.; Hajjar-Garreau, S.; Josien, L.; Michelin, L.; Bennici, S.; Limousy, L. Unveiling the Potential of Corn Cob Biochar: Analysis of Microstructure and Composition with Emphasis on Interaction with NO2. *Materials* **2024**, *17*, doi:10.3390/ma17010159.
48. Luo, L.; Wang, J.; Lv, J.; Liu, Z.; Sun, T.; Yang, Y.; Zhu, Y.-G. Carbon Sequestration Strategies in Soil Using Biochar: Advances, Challenges, and Opportunities. *Environ. Sci. Technol.* **2023**, *57*, 11357–11372, doi:10.1021/acs.est.3c02620.
49. Brassard, P.; Godbout, S.; Lévesque, V.; Palacios, J.H.; Raghavan, V.; Ahmed, A.; Hogue, R.; Jeanne, T.; Verma, M. 4 - Biochar for Soil Amendment. In *Char and Carbon Materials Derived from Biomass*; Jeguirim, M., Limousy, L., Eds.; Elsevier, 2019; pp. 109–146 ISBN 978-0-12-814893-8.
50. Godlewska, P.; Schmidt, H.P.; Ok, Y.S.; Oleszczuk, P. Biochar for Composting Improvement and Contaminants Reduction. A Review. *Bioresource Technology* **2017**, *246*, 193–202, doi:10.1016/j.biortech.2017.07.095.
51. Xiang, W.; Zhang, X.; Chen, J.; Zou, W.; He, F.; Hu, X.; Tsang, D.C.W.; Ok, Y.S.; Gao, B. Biochar Technology in Wastewater Treatment: A Critical Review. *Chemosphere* **2020**, *252*, 126539, doi:10.1016/j.chemosphere.2020.126539.
52. Rawat, S.; Wang, C.-T.; Lay, C.-H.; Hotha, S.; Bhaskar, T. Sustainable Biochar for Advanced Electrochemical/Energy Storage Applications. *Journal of Energy Storage* **2023**, *63*, 107115, doi:10.1016/j.est.2023.107115.
53. Qiu, B.; Shao, Q.; Shi, J.; Yang, C.; Chu, H. Application of Biochar for the Adsorption of Organic Pollutants from Wastewater: Modification Strategies, Mechanisms and Challenges. *Separation and Purification Technology* **2022**, *300*, 121925, doi:10.1016/j.seppur.2022.121925.
54. Kalu, S.; Kulmala, L.; Zrim, J.; Peltokangas, K.; Tammeorg, P.; Rasa, K.; Kitzler, B.; Pihlatie, M.; Karhu, K. Potential of Biochar to Reduce Greenhouse Gas Emissions and Increase Nitrogen Use Efficiency in Boreal Arable Soils in the Long-Term. *Frontiers in Environmental Science* **2022**, *10*, doi:10.3389/fenvs.2022.914766.
55. Jiang, T.; Wang, B.; Gao, B.; Cheng, N.; Feng, Q.; Chen, M.; Wang, S. Degradation of Organic Pollutants from Water by Biochar-Assisted Advanced Oxidation Processes: Mechanisms and Applications. *Journal of Hazardous Materials* **2023**, *442*, 130075, doi:10.1016/j.jhazmat.2022.130075.
56. Lyu, H.; Zhang, Q.; Shen, B. Application of Biochar and Its Composites in Catalysis. *Chemosphere* **2020**, *240*, 124842, doi:10.1016/j.chemosphere.2019.124842.
57. Gayathri, R.; Gopinath, K.P.; Kumar, P.S. Adsorptive Separation of Toxic Metals from Aquatic Environment Using Agro Waste Biochar: Application in Electroplating Industrial Wastewater. *Chemosphere* **2021**, *262*, 128031, doi:10.1016/j.chemosphere.2020.128031.
58. Hemavathy, R.V.; Kumar, P.S.; Kanmani, K.; Jahnavi, N. Adsorptive Separation of Cu(II) Ions from Aqueous Medium Using Thermally/Chemically Treated Cassia Fistula Based Biochar. *Journal of Cleaner Production* **2020**, *249*, 119390, doi:10.1016/j.jclepro.2019.119390.

59. El-Naggar, A.; El-Naggar, A.H.; Shaheen, S.M.; Sarkar, B.; Chang, S.X.; Tsang, D.C.W.; Rinklebe, J.; Ok, Y.S. Biochar Composition-Dependent Impacts on Soil Nutrient Release, Carbon Mineralization, and Potential Environmental Risk: A Review. *Journal of Environmental Management* **2019**, *241*, 458–467, doi:10.1016/j.jenvman.2019.02.044.
60. El-Naggar, A.; Lee, S.S.; Rinklebe, J.; Farooq, M.; Song, H.; Sarmah, A.K.; Zimmerman, A.R.; Ahmad, M.; Shaheen, S.M.; Ok, Y.S. Biochar Application to Low Fertility Soils: A Review of Current Status, and Future Prospects. *Geoderma* **2019**, *337*, 536–554, doi:10.1016/j.geoderma.2018.09.034.
61. Hu, X.; Xu, J.; Wu, M.; Xing, J.; Bi, W.; Wang, K.; Ma, J.; Liu, X. Effects of Biomass Pre-Pyrolysis and Pyrolysis Temperature on Magnetic Biochar Properties. *Journal of Analytical and Applied Pyrolysis* **2017**, *127*, 196–202, doi:10.1016/j.jaap.2017.08.006.
62. Senthil Kumar, P.; Abhinaya, R.V.; Gayathri Lashmi, K.; Arthi, V.; Pavithra, R.; Sathyaselvabala, V.; Dinesh Kirupha, S.; Sivanesan, S. Adsorption of Methylene Blue Dye from Aqueous Solution by Agricultural Waste: Equilibrium, Thermodynamics, Kinetics, Mechanism and Process Design. *Colloid Journal* **2011**, *73*, 651–661, doi:10.1134/S1061933X11050061.
63. Kumar, P.S.; Senthamarai, C.; Deepthi, A.S.L.S.; Bharani, R. Adsorption Isotherms, Kinetics and Mechanism of Pb(II) Ions Removal from Aqueous Solution Using Chemically Modified Agricultural Waste. *Canadian Journal of Chemical Engineering* **2013**, *91*, 1950–1956.
64. Varjani, S.; Kumar, G.; Rene, E.R. Developments in Biochar Application for Pesticide Remediation: Current Knowledge and Future Research Directions. *Journal of Environmental Management* **2019**, *232*, 505–513, doi:10.1016/j.jenvman.2018.11.043.
65. Bridgwater, A.V. Review of Fast Pyrolysis of Biomass and Product Upgrading. *Biomass and Bioenergy* **2012**, *38*, 68–94, doi:10.1016/j.biombioe.2011.01.048.
66. Ng, W.C.; You, S.; Ling, R.; Gin, K.Y.-H.; Dai, Y.; Wang, C.-H. Co-Gasification of Woody Biomass and Chicken Manure: Syngas Production, Biochar Reutilization, and Cost-Benefit Analysis. *Energy* **2017**, *139*, 732–742, doi:10.1016/j.energy.2017.07.165.
67. Cantrell, K.B.; Hunt, P.G.; Uchimiya, M.; Novak, J.M.; Ro, K.S. Impact of Pyrolysis Temperature and Manure Source on Physicochemical Characteristics of Biochar. *Bioresource Technology* **2012**, *107*, 419–428, doi:10.1016/j.biortech.2011.11.084.
68. Funke, A.; Ziegler, F. Hydrothermal Carbonization of Biomass: A Summary and Discussion of Chemical Mechanisms for Process Engineering. *Biofuels, Bioproducts and Biorefining* **2010**, *4*, 160–177, doi:10.1002/bbb.198.
69. Klinghoffer, N.B.; Castaldi, M.J.; Nzihou, A. Influence of Char Composition and Inorganics on Catalytic Activity of Char from Biomass Gasification. *Fuel* **2015**, *157*, 37–47, doi:10.1016/j.fuel.2015.04.036.
70. P.C.A. Bergman, A.R. Boersma, R.W.R. Zwart, J.H.A. Kiel, Torrefaction for Biomass Co-Firing in Existing Coal-Fired Power Stations; Report No. ECNC05013, Energy Research Centre of The Netherlands (ECN), Petten, The Netherlands, 2005, pp. 71.
71. Nunoura, T.; Wade, S.R.; Bourke, J.P.; Antal, M.J. Studies of the Flash Carbonization Process. 1. Propagation of the Flaming Pyrolysis Reaction and Performance of a Catalytic Afterburner. *Ind. Eng. Chem. Res.* **2006**, *45*, 585–599, doi:10.1021/ie050854y.
72. Basu, P. Chapter 5 - Pyrolysis. In *Biomass Gasification, Pyrolysis and Torrefaction (Third Edition)*; Basu, P., Ed.; Academic Press, 2018; pp. 155–187 ISBN 978-0-12-812992-0.
73. Devi, M.; Rawat, S.; Sharma, S. A Comprehensive Review of the Pyrolysis Process: From Carbon Nanomaterial Synthesis to Waste Treatment. *Oxford Open Materials Science* **2021**, *1*, itab014, doi:10.1093/oxfmat/itab014.
74. Cha, J.S.; Park, S.H.; Jung, S.-C.; Ryu, C.; Jeon, J.-K.; Shin, M.-C.; Park, Y.-K. Production and Utilization of Biochar: A Review. *Journal of Industrial and Engineering Chemistry* **2016**, *40*, 1–15, doi:10.1016/j.jiec.2016.06.002.
75. Yaashikaa, P.R.; Senthil Kumar, P.; Varjani, S.J.; Saravanan, A. Advances in Production and Application of Biochar from Lignocellulosic Feedstocks for Remediation of Environmental Pollutants. *Bioresource Technology* **2019**, *292*, 122030, doi:10.1016/j.biortech.2019.122030.
76. Gontijo, L.O.L.; Junior, M.N.B.; Santos de Sá, D.; Letichevsky, S.; Pedrozo-Peñafiel, M.J.; Aucélio, R.Q.; Bott, I.S.; Diniz Lopes Alves, H.; Fragneaud, B.; Oliveira Maciel, I.; et al. 3D Conductive Monolithic Carbons from Pyrolyzed Bamboo for Microfluidic Self-Heating System. *Carbon* **2023**, *213*, 118214, doi:10.1016/j.carbon.2023.118214.

77. Swagathnath, G.; Rangabhashiyam, S.; Parthsarathi, K.; Murugan, S.; Balasubramanian, P. Modeling Biochar Yield and Syngas Production During the Pyrolysis of Agro-Residues. In Proceedings of the Green Buildings and Sustainable Engineering; Drück, H., Pillai, R.G., Tharian, M.G., Majeed, A.Z., Eds.; Springer Singapore: Singapore, 2019; pp. 325–336.
78. Ibitoye, S.E.; Mahamood, R.M.; Jen, T.-C.; Loha, C.; Akinlabi, E.T. An Overview of Biomass Solid Fuels: Biomass Sources, Processing Methods, and Morphological and Microstructural Properties. *Journal of Bioresources and Bioproducts* **2023**, *8*, 333–360, doi:10.1016/j.jobab.2023.09.005.
79. Tan, H.; et al. A Review On The Comparison Between Slow Pyrolysis And Fast Pyrolysis On The Quality Of Lignocellulosic And Lignin-Based Biochar *IOP Conf. Ser.: Mater. Sci. Eng.* **2021**, *1051* 012075. DOI 10.1088/1757-899X/1051/1/012075.
80. Kumar, A.; Bhattacharya, T. *Biochar and Its Application* **2018**.
81. Tomczyk, A.; Sokołowska, Z.; Boguta, P. Biochar Physicochemical Properties: Pyrolysis Temperature and Feedstock Kind Effects. *Reviews in Environmental Science and Bio/Technology* **2020**, *19*, 191–215, doi:10.1007/s11157-020-09523-3.
82. Ding, W.; Dong, X.; Ime, I.M.; Gao, B.; Ma, L.Q. Pyrolytic Temperatures Impact Lead Sorption Mechanisms by Bagasse Biochars. *Chemosphere* **2014**, *105*, 68–74, doi:10.1016/j.chemosphere.2013.12.042.
83. Banik, C.; Lawrinenko, M.; Bakshi, S.; Laird, D.A. Impact of Pyrolysis Temperature and Feedstock on Surface Charge and Functional Group Chemistry of Biochars. *Journal of Environmental Quality* **2018**, *47*, 452–461, doi:10.2134/jeq2017.11.0432.
84. Zhao, S.-X.; Ta, N.; Wang, X.-D. Effect of Temperature on the Structural and Physicochemical Properties of Biochar with Apple Tree Branches as Feedstock Material. *Energies* **2017**, *10*, doi:10.3390/en10091293.
85. Suliman, W.; Harsh, J.B.; Abu-Lail, N.I.; Fortuna, A.-M.; Dallmeyer, I.; Garcia-Pérez, M. The Role of Biochar Porosity and Surface Functionality in Augmenting Hydrologic Properties of a Sandy Soil. *Science of The Total Environment* **2017**, *574*, 139–147, doi:10.1016/j.scitotenv.2016.09.025.
86. Gontijo, L.O.; Junior, M.N.B.; de Sá, D.S.; Letichevsky, S.; Pedrozo-Peñafiel, M.J.; Aucélio, R.Q.; ... Pandoli, O.G. 3D conductive monolithic carbons from pyrolyzed bamboo for microfluidic self-heating system. *Carbon*, **2023**, 118214.
87. Sudarsan, J.S.; Prasanna, K.; Shiam Babu, R.; Sai Krishna, V.M.V. Chapter 11 - Biochar: A Sustainable Solution for Organic Waste Management a Way Forward towards Circular Economy. In *Recent Trends in Solid Waste Management*; Ravindran, B., Gupta, S.K., Bhat, S.A., Chauhan, P.S., Tyagi, N., Eds.; Elsevier, 2023; pp. 215–230 ISBN 978-0-443-15206-1.
88. Zhou, B.; Liu, Q.; Shi, L.; Liu, Z. Electron Spin Resonance Studies of Coals and Coal Conversion Processes: A Review. *Fuel Processing Technology* **2019**, *188*, 212–227, doi:10.1016/j.fuproc.2019.01.011.
89. Zhang, S.; Cui, J.; Wu, H.; Zheng, Q.; Song, D.; Wang, X.; Zhang, S. Organic Carbon, Total Nitrogen, and Microbial Community Distributions within Aggregates of Calcareous Soil Treated with Biochar. *Agriculture, Ecosystems & Environment* **2021**, *314*, 107408, doi:10.1016/j.agee.2021.107408.
90. Ma, L.; Song, D.; Liu, M.; Li, Y.; Li, Y. Effects of Earthworm Activities on Soil Nutrients and Microbial Diversity under Different Tillage Measures. *Soil and Tillage Research* **2022**, *222*, 105441, doi:10.1016/j.still.2022.105441.
91. Hu, W.; Gao, W.; Tang, Y.; Zhang, Q.; Tu, C.; Cheng, J. Remediation via Biochar and Potential Health Risk of Heavy Metal Contaminated Soils. *Environmental Earth Sciences* **2022**, *81*, 482.
92. Kant Bhatia, S.; Palai, A.K.; Kumar, A.; Kant Bhatia, R.; Kumar Patel, A.; Kumar Thakur, V.; Yang, Y.-H. Trends in Renewable Energy Production Employing Biomass-Based Biochar. *Bioresource Technology* **2021**, *340*, 125644, doi:10.1016/j.biortech.2021.125644.
93. Sakhiya, A.K.; Anand, A.; Kaushal, P. Production, Activation, and Applications of Biochar in Recent Times. *Biochar* **2020**, 1–33.
94. Nguyen, H.N.; Pignatello, J.J. Laboratory Tests of Biochars as Absorbents for Use in Recovery or Containment of Marine Crude Oil Spills. *Environmental Engineering Science* **2013**, *30*, 374–380, doi:10.1089/ees.2012.0411.
95. Jothirani, R.; Kumar, P.S.; Saravanan, A.; Narayan, A.S.; Dutta, A. Ultrasonic Modified Corn Pith for the Sequestration of Dye from Aqueous Solution. *Journal of Industrial and Engineering Chemistry* **2016**, *39*, 162–175, doi:10.1016/j.jiec.2016.05.024.
96. Suganya, S.; Senthil Kumar, P.; Saravanan, A.; Sundar Rajan, P.; Ravikumar, C. Computation of Adsorption Parameters for the Removal of Dye from Wastewater by Microwave Assisted Sawdust: Theoretical and

Experimental Analysis. *Environmental Toxicology and Pharmacology* **2017**, *50*, 45–57, doi:10.1016/j.etap.2017.01.014.

97. Saravanan, A.; Kumar, P.S.; Renita, A.A. Hybrid Synthesis of Novel Material through Acid Modification Followed Ultrasonication to Improve Adsorption Capacity for Zinc Removal. *Journal of Cleaner Production* **2018**, *172*, 92–105, doi:10.1016/j.jclepro.2017.10.109.
98. Luo, Z.; Yao, B.; Yang, X.; Wang, L.; Xu, Z.; Yan, X.; Tian, L.; Zhou, H.; Zhou, Y. Novel Insights into the Adsorption of Organic Contaminants by Biochar: A Review. *Chemosphere* **2022**, *287*, 132113, doi:10.1016/j.chemosphere.2021.132113.
99. Lou, L.; Wu, B.; Wang, L.; Luo, L.; Xu, X.; Hou, J.; Xun, B.; Hu, B.; Chen, Y. Sorption and Ecotoxicity of Pentachlorophenol Polluted Sediment Amended with Rice-Straw Derived Biochar. *Bioresource Technology* **2011**, *102*, 4036–4041, doi:10.1016/j.biortech.2010.12.010.
100. Tan, X.; Liu, Y.; Zeng, G.; Wang, X.; Hu, X.; Gu, Y.; Yang, Z. Application of Biochar for the Removal of Pollutants from Aqueous Solutions. *Chemosphere* **2015**, *125*, 70–85, doi:10.1016/j.chemosphere.2014.12.058.
101. Yu, X.-Y.; Ying, G.-G.; Kookana, R.S. Reduced Plant Uptake of Pesticides with Biochar Additions to Soil. *Chemosphere* **2009**, *76*, 665–671, doi:10.1016/j.chemosphere.2009.04.001.
102. Liang, C.; Niu, H.-Y.; Guo, H.; Niu, C.-G.; Yang, Y.-Y.; Liu, H.-Y.; Tang, W.-W.; Feng, H.-P. Efficient Photocatalytic Nitrogen Fixation to Ammonia over Bismuth Monoxide Quantum Dots-Modified Defective Ultrathin Graphitic Carbon Nitride. *Chemical Engineering Journal* **2021**, *406*, 126868, doi:10.1016/j.cej.2020.126868.
103. Kumbhar, D.; Palliyarayil, A.; Reghu, D.; Shrungar, D.; Umapathy, S.; Sil, S. Rapid Discrimination of Porous Bio-Carbon Derived from Nitrogen Rich Biomass Using Raman Spectroscopy and Artificial Intelligence Methods. *Carbon* **2021**, *178*, 792–802, doi:10.1016/j.carbon.2021.03.064.
104. Zhang, K.; Sun, P.; Faye, M.C.A.S.; Zhang, Y. Characterization of Biochar Derived from Rice Husks and Its Potential in Chlorobenzene Degradation. *Carbon* **2018**, *130*, 730–740, doi:10.1016/j.carbon.2018.01.036.
105. Chen, D.; Xu, J.; Ling, P.; Fang, Z.; Ren, Q.; Xu, K.; Jiang, L.; Wang, Y.; Su, S.; Hu, S.; et al. Formation and Evolution Mechanism of Persistent Free Radicals in Biochar during Biomass Pyrolysis: Insights from Biochar's Element Composition and Chemical Structure. *Fuel* **2024**, *357*, 129910, doi:10.1016/j.fuel.2023.129910.
106. Wu, C.; Fu, L.; Li, H.; Liu, X.; Wan, C. Using Biochar to Strengthen the Removal of Antibiotic Resistance Genes: Performance and Mechanism. *Science of The Total Environment* **2022**, *816*, 151554, doi:10.1016/j.scitotenv.2021.151554.
107. Huang, C.; Qin, F.; Zhang, C.; Huang, D.; Tang, L.; Yan, M.; Wang, W.; Song, B.; Qin, D.; Zhou, Y.; et al. Effects of Heterogeneous Metals on the Generation of Persistent Free Radicals as Critical Redox Sites in Iron-Containing Biochar for Persulfate Activation. *ACS EST Water* **2023**, *3*, 298–310, doi:10.1021/acsestwater.2c00299.
108. Yu, J.; Zhu, Z.; Zhang, H.; Shen, X.; Qiu, Y.; Yin, D.; Wang, S. Persistent Free Radicals on N-Doped Hydrochar for Degradation of Endocrine Disrupting Compounds. *Chemical Engineering Journal* **2020**, *398*, 125538, doi:10.1016/j.cej.2020.125538.
109. Ma, L.; Syed-Hassan, S.S.A.; Tong, Y.; Xiong, Z.; Chen, Y.; Xu, J.; Jiang, L.; Su, S.; Hu, S.; Wang, Y.; et al. Interactions of Cellulose- and Lignin-Derived Radicals during Pyrolysis: An in-Situ Electron Paramagnetic Resonance (EPR) Study. *Fuel Processing Technology* **2023**, *239*, 107536, doi:10.1016/j.fuproc.2022.107536.
110. Retcofsky, H.L.; Hough, M.R.; Clarkson, R.B. Nature of the Free Radicals in Coals, Pyrolyzed Coals, and Liquefaction Products, 1979. Journal Volume: 24:1; Conference: 177. national meeting of the American Chemical Society, Honolulu, HI, USA, 1 Apr 1979.
111. Liu, J.; Jiang, X.; Shen, J.; Zhang, H. Chemical Properties of Superfine Pulverized Coal Particles. Part 1. Electron Paramagnetic Resonance Analysis of Free Radical Characteristics. *Advanced Powder Technology* **2014**, *25*, 916–925, doi:10.1016/j.apt.2014.01.021.
112. Luo, K.; Pang, Y.; Wang, D.; Li, X.; Wang, L.; Lei, M.; Huang, Q.; Yang, Q. A Critical Review on the Application of Biochar in Environmental Pollution Remediation: Role of Persistent Free Radicals (PFRs). *Journal of Environmental Sciences* **2021**, *108*, 201–216, doi:10.1016/j.jes.2021.02.021.
113. Zhang, Y.; Sun, X.; Bian, W.; Peng, J.; Wan, H.; Zhao, J. The Key Role of Persistent Free Radicals on the Surface of Hydrochar and Pyrocarbon in the Removal of Heavy Metal-Organic Combined Pollutants. *Bioresource Technology* **2020**, *318*, 124046, doi:10.1016/j.biortech.2020.124046.

114. Qin, J.; Cheng, Y.; Sun, M.; Yan, L.; Shen, G. Catalytic Degradation of the Soil Fumigant 1,3-Dichloropropene in Aqueous Biochar Slurry. *Science of The Total Environment* **2016**, *569–570*, 1–8, doi:10.1016/j.scitotenv.2016.06.092.
115. Huang, D.; Luo, H.; Zhang, C.; Zeng, G.; Lai, C.; Cheng, M.; Wang, R.; Deng, R.; Xue, W.; Gong, X.; et al. Nonnegligible Role of Biomass Types and Its Compositions on the Formation of Persistent Free Radicals in Biochar: Insight into the Influences on Fenton-like Process. *Chemical Engineering Journal* **2019**, *361*, 353–363, doi:10.1016/j.cej.2018.12.098.
116. Wang, Y.; Gu, X.; Huang, Y.; Ding, Z.; Chen, Y.; Hu, X. Insight into Biomass Feedstock on Formation of Biochar-Bound Environmentally Persistent Free Radicals under Different Pyrolysis Temperatures. *RSC Adv.* **2022**, *12*, 19318–19326, doi:10.1039/D2RA03052G.
117. Tao, W.; Duan, W.; Liu, C.; Zhu, D.; Si, X.; Zhu, R.; Oleszczuk, P.; Pan, B. Formation of Persistent Free Radicals in Biochar Derived from Rice Straw Based on a Detailed Analysis of Pyrolysis Kinetics. *Science of The Total Environment* **2020**, *715*, 136575, doi:10.1016/j.scitotenv.2020.136575.
118. Xiang, C.; Liu, Q.; Shi, L.; Liu, Z. A Study on the New Type of Radicals in Corncob Derived Biochars. *Fuel* **2020**, *277*, 118163, doi:10.1016/j.fuel.2020.118163.
119. Chintala, R.; Subramanian, S.; Fortuna, A.-M.; Schumacher, T.E. Examining Biochar Impacts on Soil Abiotic and Biotic Processes and Exploring the Potential for Pyrosequencing Analysis. Chapter 6, In *Biochar Application Essential Soil Microbial Ecology*, Komang Ralebitso-Senior, T.; Orr, C.H. Eds; Elsevier, 2016, pp. 133-162, ISBN 9780128034330, https://doi.org/10.1016/B978-0-12-803433-0.00006-0.
120. Takeshita, A.; Uemura, Y.; Onoe, K. Quantification of Persistent Free Radicals (PFRs) Formed in Thermally Decomposed Cellulose and Its Correlation with Residual Carbon Amount. *Journal of Analytical and Applied Pyrolysis* **2020**, *150*, 104883, doi:10.1016/j.jaap.2020.104883.
121. Pan, B.; Li, H.; Lang, D.; Xing, B. Environmentally Persistent Free Radicals: Occurrence, Formation Mechanisms and Implications. *Environmental Pollution* **2019**, *248*, 320–331, doi:10.1016/j.envpol.2019.02.032.
122. Lomnicki, S.M.; Truong, H.; Vejerano, E.P.; Dellinger, B. Copper Oxide-Based Model of Persistent Free Radical Formation on Combustion-Derived Particulate Matter. *Environmental science & technology* **2008**, *42 13*, 4982–4988.
123. Gasim, M.F.; Choong, Z.-Y.; Koo, P.-L.; Low, S.-C.; Abdurahman, M.-H.; Ho, Y.-C.; Mohamad, M.; Suryawan, I.W.; Lim, J.-W.; Oh, W.-D. Application of Biochar as Functional Material for Remediation of Organic Pollutants in Water: An Overview. *Catalysts* **2022**, *12*, doi:10.3390/catal12020210.
124. Zhong, D.; Jiang, Y.; Zhao, Z.; Wang, L.; Chen, J.; Ren, S.; Liu, Z.; Zhang, Y.; Tsang, D.C.W.; Crittenden, J.C. pH Dependence of Arsenic Oxidation by Rice-Husk-Derived Biochar: Roles of Redox-Active Moieties. *Environ. Sci. Technol.* **2019**, *53*, 9034–9044, doi:10.1021/acs.est.9b00756.
125. Zhang, K.; Sun, P.; Zhang, Y. Decontamination of Cr(VI) Facilitated Formation of Persistent Free Radicals on Rice Husk Derived Biochar. *Frontiers of Environmental Science & Engineering* **2019**, *13*, 22, doi:10.1007/s11783-019-1106-7.
126. Zhu, S.; Huang, X.; Yang, X.; Peng, P.; Li, Z.; Jin, C. Enhanced Transformation of Cr(VI) by Heterocyclic-N within Nitrogen-Doped Biochar: Impact of Surface Modulatory Persistent Free Radicals (PFRs). *Environ. Sci. Technol.* **2020**, *54*, 8123–8132, doi:10.1021/acs.est.0c02713.
127. Wang, X.; Xu, J.; Liu, J.; Liu, J.; Xia, F.; Wang, C.; Dahlgren, R.A.; Liu, W. Mechanism of Cr(VI) Removal by Magnetic Greigite/Biochar Composites. *Science of The Total Environment* **2020**, *700*, 134414, doi:10.1016/j.scitotenv.2019.134414.
128. Tang, Z.; Kong, Y.; Zhao, S.; Jia, H.; Vione, D.; Kang, Y.; Gao, P. Enhancement of Cr(VI) Decontamination by Irradiated Sludge Biochar in Neutral Conditions: Evidence of a Possible Role of Persistent Free Radicals. *Separation and Purification Technology* **2021**, *277*, 119414, doi:10.1016/j.seppur.2021.119414.
129. Zhu, Y.; Wei, J.; Li, J. Decontamination of Cr(VI) from Water Using Sewage Sludge-Derived Biochar: Role of Environmentally Persistent Free Radicals. *Chinese Journal of Chemical Engineering* **2023**, *56*, 97–103, doi:10.1016/j.cjche.2022.06.015.
130. Baltrėnaitė-Gedienė, E.; Lomnicki, S.; Guo, C. Impact of Biochar, Fertilizers and Cultivation Type on Environmentally Persistent Free Radicals in Agricultural Soil. *Environmental Technology & Innovation* **2022**, *28*, 102755, doi:10.1016/j.eti.2022.102755.
131. Tai, Y.; Sun, J.; Tian, H.; Liu, F.; Han, B.; Fu, W.; Liu, Z.; Yang, X.; Liu, Q. Efficient Degradation of Organic Pollutants by S-NaTaO3/Biochar under Visible Light and the Photocatalytic Performance of a

Permonosulfate-Based Dual-Effect Catalytic System. *Journal of Environmental Sciences* **2023**, *125*, 388–400, doi:10.1016/j.jes.2022.01.028.

132. Kelley, M.A.; Hebert, V.Y.; Thibeaux, T.M.; Orchard, M.A.; Hasan, F.; Cormier, S.A.; Thevenot, P.T.; Lomnicki, S.M.; Varner, K.J.; Dellinger, B.; et al. Model Combustion-Generated Particulate Matter Containing Persistent Free Radicals Redox Cycle to Produce Reactive Oxygen Species. *Chem. Res. Toxicol.* **2013**, *26*, 1862–1871, doi:10.1021/tx400227s.
133. Squadrito, G.L.; Cueto, R.; Dellinger, B.; Pryor, W.A. Quinoid Redox Cycling as a Mechanism for Sustained Free Radical Generation by Inhaled Airborne Particulate Matter. *Free Radical Biology and Medicine* **2001**, *31*, 1132–1138, doi:10.1016/S0891-5849(01)00703-1.
134. Alburquerque, J.A.; Salazar, P.; Barrón, V.; Torrent, J.; del Campillo, M. del C.; Gallardo, A.; Villar, R. Enhanced Wheat Yield by Biochar Addition under Different Mineral Fertilization Levels. *Agronomy for Sustainable Development* **2013**, *33*, 475–484, doi:10.1007/s13593-012-0128-3.
135. Jiang, S.-F.; Ling, L.-L.; Chen, W.-J.; Liu, W.-J.; Li, D.-C.; Jiang, H. High Efficient Removal of Bisphenol A in a Peroxymonosulfate/Iron Functionalized Biochar System: Mechanistic Elucidation and Quantification of the Contributors. *Chemical Engineering Journal* **2019**, *359*, 572–583, doi:10.1016/j.cej.2018.11.124.
136. Luo, H.; Lin, Q.; Zhang, X.; Huang, Z.; Liu, S.; Jiang, J.; Xiao, R.; Liao, X. New Insights into the Formation and Transformation of Active Species in nZVI/BC Activated Persulfate in Alkaline Solutions. *Chemical Engineering Journal* **2019**, *359*, 1215–1223, doi:10.1016/j.cej.2018.11.056.
137. Pi, Z.; Li, X.; Wang, D.; Xu, Q.; Tao, Z.; Huang, X.; Yao, F.; Wu, Y.; He, L.; Yang, Q. Persulfate Activation by Oxidation Biochar Supported Magnetite Particles for Tetracycline Removal: Performance and Degradation Pathway. *Journal of Cleaner Production* **2019**, *235*, 1103–1115, doi:10.1016/j.jclepro.2019.07.037.
138. He, J.; Xiao, Y.; Tang, J.; Chen, H.; Sun, H. Persulfate Activation with Sawdust Biochar in Aqueous Solution by Enhanced Electron Donor-Transfer Effect. *Science of The Total Environment* **2019**, *690*, 768–777, doi:10.1016/j.scitotenv.2019.07.043.
139. Danping, W.U.; Fangfang, L.I.; Jing, Z.; Peng, W.; Min, W.U. Photocatalysis degradation of rhodamine B by dissolved organic matter of biochars[J]. *Chinese Journal of Environmental Engineering* **2019**, *13(11)*, 2562-2569. doi: 10.12030/j.cjee.201811191https://doi.org/10.1016/j.cej.2019.05.204.
140. Wang, H.; Guo, W.; Yin, R.; Du, J.; Wu, Q.; Luo, H.; Liu, B.; Sseguya, F.; Ren, N. Biochar-Induced Fe(III) Reduction for Persulfate Activation in Sulfamethoxazole Degradation: Insight into the Electron Transfer, Radical Oxidation and Degradation Pathways. *Chemical Engineering Journal* **2019**, *362*, 561–569, doi:10.1016/j.cej.2019.01.053
141. Zhu, K.; Wang, X.; Geng, M.; Chen, D.; Lin, H.; Zhang, H. Catalytic Oxidation of Clofibric Acid by Peroxydisulfate Activated with Wood-Based Biochar: Effect of Biochar Pyrolysis Temperature, Performance and Mechanism. *Chemical Engineering Journal* **2019**, *374*, 1253–1263, doi:10.1016/j.cej.2019.06.006.
142. Li, L.; Lai, C.; Huang, F.; Cheng, M.; Zeng, G.; Huang, D.; Li, B.; Liu, S.; Zhang, M.; Qin, L.; et al. Degradation of Naphthalene with Magnetic Bio-Char Activate Hydrogen Peroxide: Synergism of Bio-Char and Fe–Mn Binary Oxides. *Water Research* **2019**, *160*, 238–248, doi:10.1016/j.watres.2019.05.081.
143. Luo, K.; Pang, Y.; Yang, Q.; Wang, D.; Li, X.; Wang, L.; Lei, M.; Liu, J. Enhanced Ciprofloxacin Removal by Sludge-Derived Biochar: Effect of Humic Acid. *Chemosphere* **2019**, *231*, 495–501, doi:10.1016/j.chemosphere.2019.05.151.
144. Deng, R.; Luo, H.; Huang, D.; Zhang, C. Biochar-Mediated Fenton-like Reaction for the Degradation of Sulfamethazine: Role of Environmentally Persistent Free Radicals. *Chemosphere* **2020**, *255*, 126975, doi:10.1016/j.chemosphere.2020.126975.
145. Liu, G.; Zhang, Y.; Yu, H.; Jin, R.; Zhou, J. Acceleration of Goethite-Catalyzed Fenton-like Oxidation of Ofloxacin by Biochar. *Journal of Hazardous Materials* **2020**, *397*, 122783, doi:10.1016/j.jhazmat.2020.122783.
146. Liu, B.; Guo, W.; Wang, H.; Si, Q.; Zhao, Q.; Luo, H.; Ren, N. Activation of Peroxymonosulfate by Cobalt-Impregnated Biochar for Atrazine Degradation: The Pivotal Roles of Persistent Free Radicals and Ecotoxicity Assessment. *Journal of Hazardous Materials* **2020**, *398*, 122768, doi:10.1016/j.jhazmat.2020.122768.
147. Grilla, E.; Vakros, J.; Konstantinou, I.; Manariotis, I.D.; Mantzavinos, D. Activation of Persulfate by Biochar from Spent Malt Rootlets for the Degradation of Trimethoprim in the Presence of Inorganic Ions. *Journal of Chemical Technology & Biotechnology* **2020**, *95*, 2348–2358, doi:10.1002/jctb.6513.

148. Feng, Z.; Zhou, B.; Yuan, R.; Li, H.; He, P.; Wang, F.; Chen, Z.; Chen, H. Biochar Derived from Different Crop Straws as Persulfate Activator for the Degradation of Sulfadiazine: Influence of Biomass Types and Systemic Cause Analysis. *Chemical Engineering Journal* **2022**, *440*, doi:10.1016/j.cej.2022.135669.
149. Kim, D.-G.; Ko, S.-O. Effects of Thermal Modification of a Biochar on Persulfate Activation and Mechanisms of Catalytic Degradation of a Pharmaceutical. *Chemical Engineering Journal* **2020**, *399*, 125377, doi:10.1016/j.cej.2020.125377.
150. He, W.; Zhu, Y.; Zeng, G.; Zhang, Y.; Wang, Y.; Zhang, M.; Long, H.; Tang, W. Efficient Removal of Perfluorooctanoic Acid by Persulfate Advanced Oxidative Degradation: Inherent Roles of Iron-Porphyrin and Persistent Free Radicals. *Chemical Engineering Journal* **2020**, *392*, 123640, doi:10.1016/j.cej.2019.123640.
151. Cao, W.; Zeng, C.; Guo, X.; Liu, Q.; Zhang, X.; Mameda, N. Enhanced Electrochemical Degradation of 2,4-Dichlorophenol with the Assist of Hydrochar. *Chemosphere* **2020**, *260*, 127643, doi:10.1016/j.chemosphere.2020.127643.
152. Xu, H.; Zhang, Y.; Li, J.; Hao, Q.; Li, X.; Liu, F. Heterogeneous Activation of Peroxymonosulfate by a Biochar-Supported Co3O4 Composite for Efficient Degradation of Chloramphenicols. *Environmental Pollution* **2020**, *257*, 113610, doi:10.1016/j.envpol.2019.113610.
153. Li, X.; Jia, Y.; Zhou, M.; Su, X.; Sun, J. High-Efficiency Degradation of Organic Pollutants with Fe, N Co-Doped Biochar Catalysts via Persulfate Activation. *Journal of Hazardous Materials* **2020**, *397*, 122764, doi:10.1016/j.jhazmat.2020.122764.
154. Xie, Y.; Hu, W.; Wang, X.; Tong, W.; Li, P.; Zhou, H.; Wang, Y.; Zhang, Y. Molten Salt Induced Nitrogen-Doped Biochar Nanosheets as Highly Efficient Peroxymonosulfate Catalyst for Organic Pollutant Degradation. *Environmental Pollution* **2020**, *260*, 114053, doi:10.1016/j.envpol.2020.114053.
155. Yan, J.; Yang, L.; Qian, L.; Han, L.; Chen, M. Nano-Magnetite Supported by Biochar Pyrolyzed at Different Temperatures as Hydrogen Peroxide Activator: Synthesis Mechanism and the Effects on Ethylbenzene Removal. *Environmental Pollution* **2020**, *261*, 114020, doi:10.1016/j.envpol.2020.114020.
156. Mian, M.M.; Liu, G.; Zhou, H. Preparation of N-Doped Biochar from Sewage Sludge and Melamine for Peroxymonosulfate Activation: N-Functionality and Catalytic Mechanisms. *Science of The Total Environment* **2020**, *744*, 140862, doi:10.1016/j.scitotenv.2020.140862.
157. Veiga, P.A. da S.; Schultz, J.; Matos, T.T. da S.; Fornari, M.R.; Costa, T.G.; Meurer, L.; Mangrich, A.S. Production of High-Performance Biochar Using a Simple and Low-Cost Method: Optimization of Pyrolysis Parameters and Evaluation for Water Treatment. *Journal of Analytical and Applied Pyrolysis* **2020**, *148*, 104823, doi:10.1016/j.jaap.2020.104823.
158. Sun, P.; Zhang, K.-K.; Zhang, Y.; Zhang, Y. Sunflower-Straw-Derived Biochar-Enhanced Fe（III/S2O82-System for Degradation of Benzoic Acid. *Environmental Science* **2020**, *(05)*, 2301-2309.
159. Zeng, L.; Chen, Q.; Tan, Y.; Lan, P.; Zhou, D.; Wu, M.; Liang, N.; Pan, B.; Xing, B. Dual Roles of Biochar Redox Property in Mediating 2,4-Dichlorophenol Degradation in the Presence of Fe3+ and Persulfate. *Chemosphere* **2021**, *279*, 130456, doi:10.1016/j.chemosphere.2021.130456.
160. Yang, F.; Zhu, Q.; Gao, Y.; Jian, H.; Wang, C.; Sun, H. Effects of Biochar-Dissolved Organic Matter on the Photodegradation of Sulfamethoxazole and Chloramphenicol in Biochar Solutions as Revealed by Oxygen Reduction Performances and Free Radicals. *Science of The Total Environment* **2021**, *781*, 146807, doi:10.1016/j.scitotenv.2021.146807.
161. Min, L.; Zhang, P.; Fan, M.; Xu, X.; Wang, C.; Tang, J.; Sun, H. Efficient Degradation of P-Nitrophenol by Fe@pomelo Peel-Derived Biochar Composites and Its Mechanism of Simultaneous Reduction and Oxidation Process. *Chemosphere* **2021**, *267*, 129213, doi:10.1016/j.chemosphere.2020.129213.
162. Mer, K.; Sajjadi, B.; Egiebor, Nosa.O.; Chen, W.-Y.; Mattern, Daniell.L.; Tao, W. Enhanced Degradation of Organic Contaminants Using Catalytic Activity of Carbonaceous Structures: A Strategy for the Reuse of Exhausted Sorbents. *Journal of Environmental Sciences* **2021**, *99*, 267–273, doi:10.1016/j.jes.2020.06.030.
163. Cao, Y.; Jiang, S.; Kang, X.; Zhang, H.; Zhang, Q.; Wang, L. Enhancing Degradation of Atrazine by Fe-Phenol Modified Biochar/Ferrate(VI) under Alkaline Conditions: Analysis of the Mechanism and Intermediate Products. *Chemosphere* **2021**, *285*, 131399, doi:10.1016/j.chemosphere.2021.131399.
164. Zhang, R.; Zheng, X.; Zhang, D.; Niu, X.; Ma, J.; Lin, Z.; Fu, M.; Zhou, S. Insight into the Roles of Endogenous Minerals in the Activation of Persulfate by Graphitized Biochar for Tetracycline Removal. *Science of The Total Environment* **2021**, *768*, 144281, doi:10.1016/j.scitotenv.2020.144281.

165. Yi, Y.; Luo, J.; Fang, Z. Magnetic Biochar Derived from Eichhornia Crassipes for Highly Efficient Fenton-like Degradation of Antibiotics: Mechanism and Contributions. *Journal of Environmental Chemical Engineering* **2021**, *9*, 106258, doi:10.1016/j.jece.2021.106258.
166. Zhang, Y.; Xu, M.; Liang, S.; Feng, Z.; Zhao, J. Mechanism of Persulfate Activation by Biochar for the Catalytic Degradation of Antibiotics: Synergistic Effects of Environmentally Persistent Free Radicals and the Defective Structure of Biochar. *Science of The Total Environment* **2021**, *794*, 148707, doi:10.1016/j.scitotenv.2021.148707.
167. Wang, X.; Zhang, P.; Wang, C.; Jia, H.; Shang, X.; Tang, J.; Sun, H. Metal-Rich Hyperaccumulator-Derived Biochar as an Efficient Persulfate Activator: Role of Intrinsic Metals (Fe, Mn and Zn) in Regulating Characteristics, Performance and Reaction Mechanisms. *Journal of Hazardous Materials* **2022**, *424*, 127225, doi:10.1016/j.jhazmat.2021.127225.
168. Luo Kun; Yang Chen; Li Xue; Pang Ya; Yang Qi Mn-Doped Biochar Derived from Sewage Sludge for Ciprofloxacin Degradation. *Journal of Environmental Engineering* **2022**, *148*, 04022048, doi:10.1061/(ASCE)EE.1943-7870.0002041.
169. Li, H.; Liu, Y.; Jiang, F.; Bai, X.; Li, H.; Lang, D.; Wang, L.; Pan, B. Persulfate Adsorption and Activation by Carbon Structure Defects Provided New Insights into Ofloxacin Degradation by Biochar. *Science of The Total Environment* **2022**, *806*, 150968, doi:10.1016/j.scitotenv.2021.150968.
170. Dai, Z.; Zhao, L.; Peng, S.; Yue, Z.; Zhan, X.; Wang, J. Removal of Oxytetracycline Promoted by Manganese-Doped Biochar Based on Density Functional Theory Calculations: Comprehensive Evaluation of the Effect of Transition Metal Doping. *Science of The Total Environment* **2022**, *806*, 150268, doi:10.1016/j.scitotenv.2021.150268.
171. Rangarajan, G.; Farnood, R. Role of Persistent Free Radicals and Lewis Acid Sites in Visible-Light-Driven Wet Peroxide Activation by Solid Acid Biochar Catalysts – A Mechanistic Study. *Journal of Hazardous Materials* **2022**, *438*, 129514, doi:10.1016/j.jhazmat.2022.129514.
172. An, X.; Chen, Y.; Ao, M.; Jin, Y.; Zhan, L.; Yu, B.; Wu, Z.; Jiang, P. Sequential Photocatalytic Degradation of Organophosphorus Pesticides and Recovery of Orthophosphate by Biochar/α-Fe2O3/MgO Composite: A New Enhanced Strategy for Reducing the Impacts of Organophosphorus from Wastewater. *Chemical Engineering Journal* **2022**, *435*, 135087, doi:10.1016/j.cej.2022.135087.
173. Jiang, Xinyi and Xiao, Ye and Xiao, Jiana and Zhang, Weihua and Rongliang, Qiu, The Effect of Persistent Free Radicals in Sludge Derived Biochar on the Removal of P-Chlorophenol. Available at SSRN: https://ssrn.com/abstract=3992617 (accessed on 04 January 2024).
174. Pan, Y.; Peng, Z.; Liu, Z.; Shao, B.; Liang, Q.; He, Q.; Wu, T.; Zhang, X.; Zhao, C.; Liu, Y.; et al. Activation of Peroxydisulfate by Bimetal Modified Peanut Hull-Derived Porous Biochar for the Degradation of Tetracycline in Aqueous Solution. *Journal of Environmental Chemical Engineering* **2022**, *10*, 107366, doi:10.1016/j.jece.2022.107366.
175. Yin, Q.; Yan, H.; Liang, Y.; Jiang, Z.; Wang, H.; Nian, Y. Activation of Persulfate by Blue Algae Biochar Supported FeOX Particles for Tetracycline Degradation: Performance and Mechanism. *Separation and Purification Technology* **2023**, *319*, 124005, doi:10.1016/j.seppur.2023.124005.
176. Badiger, S.M.; Nidheesh, P.V. Applications of Biochar in Sulfate Radical-Based Advanced Oxidation Processes for the Removal of Pharmaceuticals and Personal Care Products. *Water Science and Technology* **2023**, *87*, 1329–1348, doi:10.2166/wst.2023.069.
177. Yu, Y.; Zhong, Z.; Guo, H.; Yu, Y.; Zheng, T.; Li, H.; Chang, Z. Biochar–Goethite Composites Inhibited/Enhanced Degradation of Triphenyl Phosphate by Activating Persulfate: Insights on the Mechanism. *Science of The Total Environment* **2023**, *858*, 159940, doi:10.1016/j.scitotenv.2022.159940.
178. Pei, S.; Zhao, Y.; Li, W.; Qu, C.; Ren, Y.; Yang, Y.; Liu, J.; Wu, C. Critical Impact of Pyrolysis Temperatures on Biochars for Peroxymonosulfate Activation: Structural Characteristics, Degradation Performance and Mechanism. *Chemical Engineering Journal* **2023**, *477*, 147274, doi:10.1016/j.cej.2023.147274.
179. Zhang, Y.; He, R.; Zhao, J.; Zhang, X.; Bildyukevich, A.V. Effect of Aged Biochar after Microbial Fermentation on Antibiotics Removal: Key Roles of Microplastics and Environmentally Persistent Free Radicals. *Bioresource Technology* **2023**, *374*, 128779, doi:10.1016/j.biortech.2023.128779.
180. Yang, Z.; An, Q.; Deng, S.; Xu, B.; Li, Z.; Deng, S.; Zhao, B.; Ye, Z. Efficient Activation of Peroxydisulfate by Modified Red Mud Biochar Derived from Waste Corn Straw for Levofloxacin Degradation: Efficiencies and Mechanisms. *Journal of Environmental Chemical Engineering* **2023**, *11*, 111609, doi:10.1016/j.jece.2023.111609.

181. Zhang, Y.; He, R.; Zhao, J. Removal Mechanism of Tetracycline-Cr(Ⅵ) Combined Pollutants by Different S-Doped Sludge Biochars: Role of Environmentally Persistent Free Radicals. *Chemosphere* **2023**, *317*, doi:10.1016/j.chemosphere.2023.137856.
182. Luo, K.; Lin, N.; Li, X.; Pang, Y.; Wang, L.; Lei, M.; Yang, Q. Efficient Hexavalent Chromium Removal by Nano-Cerium Oxide Functionalized Biochar: Insight into the Role of Reduction. *Journal of Environmental Chemical Engineering* **2023**, *11*, 110004, doi:10.1016/j.jece.2023.110004.
183. Zhong, D.; Zhao, Z.; Jiang, Y.; Yang, X.; Wang, L.; Chen, J.; Guan, C.-Y.; Zhang, Y.; Tsang, D.C.W.; Crittenden, J.C. Contrasting Abiotic As(III) Immobilization by Undissolved and Dissolved Fractions of Biochar in Ca2+-Rich Groundwater under Anoxic Conditions. *Water Research* **2020**, *183*, 116106, doi:10.1016/j.watres.2020.116106.
184. Huang, Y.; Gao, M.; Deng, Y.; Khan, Z.H.; Liu, X.; Song, Z.; Qiu, W. Efficient Oxidation and Adsorption of As(III) and As(V) in Water Using a Fenton-like Reagent, (Ferrihydrite)-Loaded Biochar. *Science of The Total Environment* **2020**, *715*, 136957, doi:10.1016/j.scitotenv.2020.136957.
185. Zhu, Y.; Wei, J.; Li, J. Biochar-Activated Persulfate Oxidation of Arsenic(III): Nonnegligible Roles of Environmentally Persistent Free Radicals. *Journal of Environmental Chemical Engineering* **2023**, *11*, 111033, doi:10.1016/j.jece.2023.111033.
186. Yu, J.; Zhu, Z.; Zhang, H.; Chen, T.; Qiu, Y.; Xu, Z.; Yin, D. Efficient Removal of Several Estrogens in Water by Fe-Hydrochar Composite and Related Interactive Effect Mechanism of H2O2 and Iron with Persistent Free Radicals from Hydrochar of Pinewood. *Science of The Total Environment* **2019**, *658*, 1013–1022, doi:10.1016/j.scitotenv.2018.12.183.
187. Zhu, N.; Li, C.; Bu, L.; Tang, C.; Wang, S.; Duan, P.; Yao, L.; Tang, J.; Dionysiou, D.D.; Wu, Y. Bismuth Impregnated Biochar for Efficient Estrone Degradation: The Synergistic Effect between Biochar and Bi/Bi2O3 for a High Photocatalytic Performance. *Journal of Hazardous Materials* **2020**, *384*, 121258, doi:10.1016/j.jhazmat.2019.121258.
188. Chen, Y.; Duan, X.; Zhang, C.; Wang, S.; Ren, N.; Ho, S.-H. Graphitic Biochar Catalysts from Anaerobic Digestion Sludge for Nonradical Degradation of Micropollutants and Disinfection. *Chemical Engineering Journal* **2020**, *384*, 123244, doi:10.1016/j.cej.2019.123244.
189. Xu, H.; Han, Y.; Wang, G.; Deng, P.; Feng, L. Walnut Shell Biochar Based Sorptive Remediation of Estrogens Polluted Simulated Wastewater: Characterization, Adsorption Mechanism and Degradation by Persistent Free Radicals. *Environmental Technology & Innovation* **2022**, *28*, 102870, doi:10.1016/j.eti.2022.102870.
190. Wang, T.; Zheng, J.; Cai, J.; Liu, Q.; Zhang, X. Visible-Light-Driven Photocatalytic Degradation of Dye and Antibiotics by Activated Biochar Composited with K+ Doped g-C3N4: Effects, Mechanisms, Actual Wastewater Treatment and Disinfection. *Science of the Total Environment* **2022**, *839*, doi:10.1016/j.scitotenv.2022.155955.
191. Shi, J.; Wang, J.; Liang, L.; Xu, Z.; Chen, Y.; Chen, S.; Xu, M.; Wang, X.; Wang, S. Carbothermal Synthesis of Biochar-Supported Metallic Silver for Enhanced Photocatalytic Removal of Methylene Blue and Antimicrobial Efficacy. *Journal of Hazardous Materials* **2021**, *401*, 123382, doi:10.1016/j.jhazmat.2020.123382.
192. Lian, F.; Yu, W.; Zhou, Q.; Gu, S.; Wang, Z.; Xing, B. Size Matters: Nano-Biochar Triggers Decomposition and Transformation Inhibition of Antibiotic Resistance Genes in Aqueous Environments. *Environ. Sci. Technol.* **2020**, *54*, 8821–8829, doi:10.1021/acs.est.0c02227.
193. Liang, Z.; Min, W.U.; Guo-juan, W.U. Electron exchange capacity of rice biochar at different preparation temperatures[J]. *CHINA ENVIRONMENTAL SCIENCECE*, **2019**, *39(10)*, 4329-4336.
194. Xiang, L.; Liu, S.; Ye, S.; Yang, H.; Song, B.; Qin, F.; Shen, M.; Tan, C.; Zeng, G.; Tan, X. Potential Hazards of Biochar: The Negative Environmental Impacts of Biochar Applications. *Journal of Hazardous Materials* **2021**, *420*, 126611, doi:10.1016/j.jhazmat.2021.126611.
195. Kharisov, B.I.; Kharissova, O.V. Carbon Allotropes in the Environment and Their Toxicity. In *Carbon Allotropes: Metal-Complex Chemistry, Properties and Applications*. Springer, Cham, 2019. https://doi.org/10.1007/978-3-030-03505-1_9.
196. El-Naggar, A.; Lee, M.-H.; Hur, J.; Lee, Y.H.; Igalavithana, A.D.; Shaheen, S.M.; Ryu, C.; Rinklebe, J.; Tsang, D.C.W.; Ok, Y.S. Biochar-Induced Metal Immobilization and Soil Biogeochemical Process: An Integrated Mechanistic Approach. *Science of The Total Environment* **2020**, *698*, 134112, doi:10.1016/j.scitotenv.2019.134112.

197. Cui, H.; Li, D.; Liu, X.; Fan, Y.; Zhang, X.; Zhang, S.; Zhou, J.; Fang, G.; Zhou, J. Dry-Wet and Freeze-Thaw Aging Activate Endogenous Copper and Cadmium in Biochar. *Journal of Cleaner Production* **2021**, *288*, 125605, doi:10.1016/j.jclepro.2020.125605.
198. Rombolà, A.G.; Fabbri, D.; Baronti, S.; Vaccari, F.P.; Genesio, L.; Miglietta, F. Changes in the Pattern of Polycyclic Aromatic Hydrocarbons in Soil Treated with Biochar from a Multiyear Field Experiment. *Chemosphere* **2019**, *219*, 662–670, doi:10.1016/j.chemosphere.2018.11.178.
199. Joseph, S.; Camps-Arbestain, M.; Lin, Y.; Munroe, P.; Chia, C.H.; Hook, J.M.; Zwieten, L.V.; Kimber, S.; Cowie, A.L.; Singh, B.P.; et al. An Investigation into the Reactions of Biochar in Soil. *Soil Research* **2010**, *48*, 501–515.
200. Kim, H.-B.; Kim, S.-H.; Jeon, E.-K.; Kim, D.-H.; Tsang, D.C.W.; Alessi, D.S.; Kwon, E.E.; Baek, K. Effect of Dissolved Organic Carbon from Sludge, Rice Straw and Spent Coffee Ground Biochar on the Mobility of Arsenic in Soil. *Science of The Total Environment* **2018**, *636*, 1241–1248, doi:10.1016/j.scitotenv.2018.04.406.
201. Jia, C.; Luo, J.; Fan, J.; Clark, J.H.; Zhang, S.; Zhu, X. Urgently Reveal Longly Hidden Toxicant in a Familiar Fabrication Process of Biomass-Derived Environment Carbon Material. *Journal of Environmental Sciences* **2021**, *100*, 250–256, doi:10.1016/j.jes.2020.08.001.
202. Liu, J.; Gao, N.; Wen, X.; Jia, H.; Lichtfouse, E. Plant and Algal Toxicity of Persistent Free Radicals and Reactive Oxygen Species Generated by Heating Anthracene-Contaminated Soils from 100 to 600 °C. *Environmental Chemistry Letters* **2021**, *19*, 2695–2703, doi:10.1007/s10311-021-01193-z.
203. Xu, Y.; Lu, X.; Su, G.; Chen, X.; Meng, J.; Li, Q.; Wang, C.; Shi, B. Scientific and Regulatory Challenges of Environmentally Persistent Free Radicals: From Formation Theory to Risk Prevention Strategies. *Journal of Hazardous Materials* **2023**, *456*, 131674, doi:10.1016/j.jhazmat.2023.131674.
204. Yi, J.-F.; Lin, Z.-Z.; Li, X.; Zhou, Y.-Q.; Guo, Y. A Short Review on Environmental Distribution and Toxicity of the Environmentally Persistent Free Radicals. *Chemosphere* **2023**, *340*, 139922, doi:10.1016/j.chemosphere.2023.139922.
205. Jaligama, S.; Patel, V.S.; Wang, P.; Sallam, A.; Harding, J.; Kelley, M.; Mancuso, S.R.; Dugas, T.R.; Cormier, S.A. Radical Containing Combustion Derived Particulate Matter Enhance Pulmonary Th17 Inflammation via the Aryl Hydrocarbon Receptor. *Particle and Fibre Toxicology* **2018**, *15*, 20, doi:10.1186/s12989-018-0255-3.
206. Harmon, A.C.; Hebert, V.Y.; Cormier, S.A.; Subramanian, B.; Reed, J.R.; Backes, W.L.; Dugas, T.R. Particulate Matter Containing Environmentally Persistent Free Radicals Induces AhR-Dependent Cytokine and Reactive Oxygen Species Production in Human Bronchial Epithelial Cells. *PLOS ONE* **2018**, *13*, e0205412, doi:10.1371/journal.pone.0205412.
207. Reed, J.R.; dela Cruz, A.L.N.; Lomnicki, S.M.; Backes, W.L. Environmentally Persistent Free Radical-Containing Particulate Matter Competitively Inhibits Metabolism by Cytochrome P450 1A2. *Toxicology and Applied Pharmacology* **2015**, *289*, 223–230, doi:10.1016/j.taap.2015.09.021.
208. Chuang, G.C.; Xia, H.; Mahne, S.E.; Varner, K.J. Environmentally Persistent Free Radicals Cause Apoptosis in HL-1 Cardiomyocytes. *Cardiovascular Toxicology* **2017**, *17*, 140–149, doi:10.1007/s12012-016-9367-x.
209. Zhao, S.; Miao, D.; Zhu, K.; Kelin, T.; Wang, C.; Sharma, V.; Jia, H. Interaction of Benzo[a]Pyrene with Cu(II)-Montmorillonite: Generation and Toxicity of Environmentally Persistent Free Radicals and Reactive Oxygen Species. *Environment International* **2019**, *129*, 154–163, doi:10.1016/j.envint.2019.05.037.
210. Thevenot, P.; Saravia, J.; Jin, N.; Giaimo, J.; Chustz, R.; Mahne, S.; Kelley, M.; Hebert, V.; Dellinger, B.; Dugas, T.; et al. Radical-Containing PM0.2 Initiates Epithelial-to-Mesenchymal Transitions in Airway Epithelial Cells. *American journal of respiratory cell and molecular biology* **2012**, *48*, doi:10.1165/rcmb.2012-0052OC.
211. Zhang, X.; Gu, W.; Ma, Z.; Liu, Y.; Ru, H.; Zhou, J.; Zang, Y.; Xu, Z.; Qian, G. Short-Term Exposure to ZnO/MCB Persistent Free Radical Particles Causes Mouse Lung Lesions via Inflammatory Reactions and Apoptosis Pathways. *Environmental Pollution* **2020**, *261*, 114039, doi:10.1016/j.envpol.2020.114039.
212. Balakrishna, S.; Saravia, J.; Thevenot, P.; Ahlert, T.; Lominiki, S.; Dellinger, B.; Cormier, S.A. Environmentally Persistent Free Radicals Induce Airway Hyperresponsiveness in Neonatal Rat Lungs. *Particle and Fibre Toxicology* **2011**, *8*, 11, doi:10.1186/1743-8977-8-11.
213. Huang, H.-S.; Ma, M.-C.; Chen, J.; Chen, C.-F. Changes in Renal Hemodynamics and Urodynamics in Rats with Chronic Hyperoxaluria and after Acute Oxalate Infusion: Role of Free Radicals. *Neurourology and Urodynamics* **2003**, *22*, 176–182, doi:10.1002/nau.10055.

214. Reinke, L.A.; Moore, D.R.; Nanji, A.A. Pronounced Hepatic Free Radical Formation Precedes Pathological Liver Injury in Ethanol-Fed Rats. *Alcoholism: Clinical and Experimental Research* **2000**, *24*, 332–335, doi:10.1111/j.1530-0277.2000.tb04615.x.
215. Burn, B.R.; Varner, K.J. Environmentally Persistent Free Radicals Compromise Left Ventricular Function during Ischemia/Reperfusion Injury. *American Journal of Physiology-Heart and Circulatory Physiology* **2015**, *308*, H998–H1006, doi:10.1152/ajpheart.00891.2014.
216. Wang, P.; You, D.; Saravia, J.; Shen, H.; Cormier, S.A. Maternal Exposure to Combustion Generated PM Inhibits Pulmonary Th1 Maturation and Concomitantly Enhances Postnatal Asthma Development in Offspring. *Particle and Fibre Toxicology* **2013**, *10*, 29, doi:10.1186/1743-8977-10-29.
217. Guan, X.; Truong, L.; Lomnicki, S.; Tanguay, R.; Cormier, S. Developmental Hazard of Environmentally Persistent Free Radicals and Protective Effect of TEMPOL in Zebrafish Model. *Toxics* **2021,** *9*, p12.
218. Zhang, Y.; Guo, X.; Si, X.; Yang, R.; Zhou, J.; Quan, X. Environmentally Persistent Free Radical Generation on Contaminated Soil and Their Potential Biotoxicity to Luminous Bacteria. *Science of The Total Environment* **2019**, *687*, 348–354, doi:10.1016/j.scitotenv.2019.06.137.
219. Zhang, X.; Chen, Y.; Hu, D.; Zhao, L.; Wang, L.; Wu, M. Neurotoxic effect of environmental persistent free radicals in rice biochar to Caenorhabditis elegans. *China Environ. Sci.* **2019**, *39*, 2644-2651.
220. Stephenson, E.J.; Ragauskas, A.; Jaligama, S.; Redd, J.R.; Parvathareddy, J.; Peloquin, M.J.; Saravia, J.; Han, J.C.; Cormier, S.A.; Bridges, D. Exposure to Environmentally Persistent Free Radicals during Gestation Lowers Energy Expenditure and Impairs Skeletal Muscle Mitochondrial Function in Adult Mice. *American Journal of Physiology-Endocrinology and Metabolism* **2016**, *310*, E1003–E1015, doi:10.1152/ajpendo.00521.2015.
221. Lee, G.I.; Saravia, J.; You, D.; Shrestha, B.; Jaligama, S.; Hebert, V.Y.; Dugas, T.R.; Cormier, S.A. Exposure to Combustion Generated Environmentally Persistent Free Radicals Enhances Severity of Influenza Virus Infection. *Part Fibre Toxicol* **2014**, *11*, 57, doi:10.1186/s12989-014-0057-1.
222. Briedé, J.J.; Godschalk, R.W.L.; Emans, M.T.G.; de Kok, T.M.C.M.; van Agen, E.; van Maanen, J.M.S.; van Schooten, F.-J.; Kleinjans, J.C.S. In Vitro and In Vivo Studies on Oxygen Free Radical and DNA Adduct Formation in Rat Lung and Liver during Benzo[a]Pyrene Metabolism. *Free Radical Research* **2004**, *38*, 995–1002, doi:10.1080/10715760400000976.
223. Balakrishna, S.; Lomnicki, S.; McAvey, K.M.; Cole, R.B.; Dellinger, B.; Cormier, S.A. Environmentally Persistent Free Radicals Amplify Ultrafine Particle Mediated Cellular Oxidative Stress and Cytotoxicity. *Particle and Fibre Toxicology* **2009**, *6*, 11, doi:10.1186/1743-8977-6-11.